STUDY OF VANADATE AS A PHOTOSENSITIZER AND KINETIC INHIBITOR OF BEEF HEART MITOCHONDRIAL F_1-ATPase

by

Mandy C. C. Kao
B.Sc. (Honors), Simon Fraser University, 1988

A THESIS SUBMITTED IN PARTIAL FULFILLMENT OF
THE REQUIREMENTS FOR THE DEGREE OF
MASTER OF SCIENCE

in the Department
of
Chemistry

SIMON FRASER UNIVERSITY
September 1990

Approval

Name: Mandy C. C. Kao

Degree: M. Sc. Chemistry

Title of thesis: Study of Vanadate as a Photosensitizer and Kinetic Inhibitor of Beef Heart Mitochondrial F_1-ATPase

Examining Committee:

Chairman: Dr. P. Percival

Dr. T. Borgford
Senior Supervisor

Dr. M. J. Gresser

Dr. R. -M. Cornell

Dr. A. S. Tracey

Dr. Haunerland

Date Approved: Dec. 7, 1990

PARTIAL COPYRIGHT LICENSE

I hereby grant to Simon Fraser University the right to lend my thesis, project or extended essay (the title of which is shown below) to users of the Simon Fraser University Library, and to make partial or single copies only for such users or in response to a request from the library of any other university, or other educational institution, on its own behalf or for one of its users. I further agree that permission for multiple copying of this work for scholarly purposes may be granted by me or the Dean of Graduate Studies. It is understood that copying or publication of this work for financial gain shall not be allowed without my written permission.

Title of Thesis/~~Project/Extended Essay~~

Study of Vanadate as a Photosensitizer and Kinetic Inhibitor of Beef Heart Mitochondrial F_1-ATPase

Author: _____
(signature)

MANDY KAO
(name)

7 DEC 1990
(date)

ABSTRACT

The ability of vanadate to act as a photosensitizing agent and also as an inhibitor of the function of beef heart mitochondrial F_1-ATPase was investigated. Vanadate-sensitized photoinactivation of F_1 was biphasic with a fast rate of inactivation followed by a less sensitive phase. Monovanadate was found to be the species interacting with F_1 during the photoinactivation process with a K_i of 12.3 ± 0.9 μM. ADP and PP_i both diminished P_i binding and Vi binding to the enzyme. ADP protected F_1 from photoinactivation whereas PP_i at concentration below 120 μM enhanced the process, but reduced the extent of photoinactivation when present in higher concentration. P_i at high concentration did not prevent vanadate-sensitized photoinactivation. Vanadate inhibited $^{32}P[P_i]$ binding to F_1 but not completely. These results suggest that P_i and Vi can bind simultaneously to the protein, and that the protein is sensitized to photoinactivation when both ligands are bound.

Electrophoresis of photoinactivated F_1 on an SDS gel showed the appearance of two new bands, P_1 and P_2, located slightly above the γ and δ bands respectively. These two bands appeared to be the products of photocleavage of the heavy subunits of F_1, but they could also be the modified γ and δ subunits with altered mobility on the SDS gel. Direct amino acid sequencing of the heavier peptide P_1 could not identify its origin because its N-terminal was ragged. Modification of β subunits also resulted from exposure of the enzyme to UV irradiation in presence of vanadate. The modified peptide had a lowered pI compared with the native

β subunits. This alteration of the protein as well as the loss in activity was not reversible by the reducing agents, $NaBH_4$ or dithiothreitol.

F_1 was inhibited by vanadate in the micromolar concentration range. NMR studies of vanadium(V) species in the assay mixture at pH 7.5 established three major forms of the vanadate in solution: mono-, di-, and tetravanadate. Analysis of results from direct kinetic inhibition studies could not identify which of the three vanadate species was the inhibitor of F_1. However, addition of P_i enhanced the inhibition of F_1-catalyzed ATP hydrolysis, and this is consistent with divanadate being one of the inhibitors.

DEDICATION

To Linda, Mom, and Dad

ACKNOWLEDGEMENTS

I would like to express my appreciations to Dr. Michael J. Gresser whose skillful guidance and encouragements were indispensable for the completion of this work. Thanks is also due to Dr. Alan S. Tracey for his assistance in the NMR work, Dr. Huali Li for providing useful information in photochemistry, Dr. Seeloch Beharry and Elithabeth Bramhall for providing F_1 and demonstration of excellent experimental techniques. I am grateful to Dr. Paul Stankiewicz for his assistance and stimulating discussions. To all members in the lab including Marcia M. Craig, Susana Liu, Dr. David Percival and Nelly Leon-Lai, I would like to thank for providing a pleasant working environment and friendship.

TABLE OF CONTENTS

Approval ii

ABSTRACT iii

DEDICATION v

ACKNOWLEDGEMENTS vi

List of Tables ix

List of Figures x

ABBREVIATIONS 1

INTRODUCTION 3

OBJECTIVES 9

EXPERIMENTAL PROCEDURES 11

MATERIALS 11

METHODS 12

RESULTS 21

Photoinactivation of F_1 in presence of vanadate 21

Effects of P_i, PP_i and ADP on photoinactivation 40

Kinetic inhibition of F_1 by vanadate 50

DISCUSSION 83

APPENDICES 92

Appendix 1 92

Appendix 2 93

REFERENCES 95

LIST OF TABLES

TABLES		PAGE
I	Effect of Presence of ADP on Vanadate-Sensitized Photoinactivation of F_1	41
IIA	NMR Determination of Formation Constants for V_2 and V_4 in Solution Containing 4.3 mM $MgCl_2$	51
IIB	NMR Determination of Formation Constants for V_2 and V_4 in Solution Containing 2 mM $MgCl_2$	52
III	Effect of P_i on F_1-Catalyzed ATP Hydrolysis	66
IV	Vanadate-Sensitized Photoinactivation of F_1 in Deoxygenated Medium	86

LIST OF FIGURES

FIGURES		PAGE
1	F_oF_1-ATPase	4
2	Time dependence of vanadate-sensitized photoinactivation of F_1	22
3	Semi-log plot of Figure 2	24
4	Double reciprocal plot of activity of photoinactivated F_1	26
5	Vanadate concentration dependence of photoinactivation of F_1	29
6	SDS-PAGE of phtoinactivated F_1	31
7	Isoelectric focusing of phtoinactivated F_1	35
8	2-D gel electrophoresis of photoinactivated F_1	37
9	Effect of presence of PP_i on vanadate-sensitized photo-inactivation of F_1	43
10	Effect of presence of P_i on vanadate-sensitized photo-inactivation of F_1	45
11	Inhibition of $^{32}P[P_i]$ binding to F_1 by vanadate	47
12	Model for simultaneous binding of P_i and Vi to F_1	49
13A	Distribution curve for Vi, V_2 and V_4 as a function of total vanadium atom concentration in solution with 4.3 mM $MgCl_2$	54
13B	Distribution curve for Vi, V_2 and V_4 as a function of total vanadium atom concentration in solution with 2 mM $MgCl_2$	54
14	The dependence of the rate of F_1-catalyzed ATP hydrolysis on MgATP concentration	56
15	Double reciprocal plots of the dependence of the rate of ATP F_1-catalyzed ATP hydrolysis on MgATP concentration at various fixed concentrations of vanadate	58
16	Secondary slope plot for Figure 15	61
17	The dependence of the rate of F_1-catalyzed ATP hydrolysis on MgATP concentration in the presence of phosphate, vanadate, or phosphate plus vanadate	64
18	Inhibition of F_1-catalyzed ATP hydrolysis by vanadate	67

19 Inhibition of F_1-catalyzed ATP hydrolysis by vanadate in presence of 10 mM P_i 69

20A Percentage inhibition of F_1-catalyzed ATP hydrolysis by vanadate as a function of vanadate concentration and in the presence of P_i --"Vanadate Effect" 72

20B Percentage inhibition of F_1-catalyzed ATP hydrolysis by vanadate as a function of vanadate concentration and in the presence of P_i -- "P_i Effect" 72

21 Apparent rate constant for dissociation of vanadate from F_1 in assay mixtures containing no vanadate or 0.5 mM vanadate 75

22 Apparent rate constant for dissociation of vanadate from F_1 as a function of substrate ATP concentration 77

23 Corrected observed rate constant of dissociation of vanadate from F_1 79

24 Model for dissociation of vanadate from F_1 81

LIST OF ABBREVIATIONS

AMP/ADP/ATP	Adenosine 5'-monophosphate/diphosphate/triphosphate
AMPPNP	5'-Adenylyl-β, γ-imidodiphosphate
ANPP	4-Azido-2-nitrophenyl phosphate
BSA	Bovine serum albumin
EF_1	F_1 ATPase from *E. coli*
F_1-BUFFER	Buffer of 150 mM sucrose/2 mM $MgSO_4$/10 mM K^+-HEPES, pH 8.0
FSBA	*p*-Fluorosulfonyl-benzoyl-5'-adenosine
FSBI	*p*-Fluorosulfonyl-benzoyl-5'-inosine
GTP	Guanosine 5'-triphosphate
HEPES	N-2-hydroxyethylpiperazine-N'-2-ethanesulfonic acid
IEF	Isoelectric focusing
LDH	Lactate dehydrogenase
MgATP/MgGTP	ATP/GTP prepared in Tris-OAc buffer with same concentration of Mg^{2+}
β-NADH	β-Nicotinamide adenine dinucleotide
Nbf-Cl	4-Chloro-7-nitrobenzofurazan
PEP	Phosphoenol pyruvate
p I	Isoelectric point
P-V	Phosphovanadate anhydride
PK	Pyruvate kinase
P_i	Inorganic phosphate
PP_i	Inorganic pyrophosphate
PVDF	Polyvinylidene difluoride

SDS-PAGE	Sodium dodecyl sulfate polyacrylamide gel electrophoresis
SOD	Superoxide dismutase
TRIS-OAc	Tris(hydroxymethyl)aminomethane buffer pH adjusted to 7.5 with acetic acid
UV	Ultraviolet
Vi	Monovanadate
V_2	Divanadate
V_4	Tetravanadate

INTRODUCTION

Mitochondrial F_1-ATPase (F_1) is the catalytic component of the ATP synthase that is involved in the terminal step of oxidative phosphorylation of ADP. The energy of the electrochemical gradient built up across the inner mitochondrial membrane is harvested in the phosphate anhydride bonds between β and γ phosphates of the ATP molecule made by this synthase (review 1, 2, 3).

Sonication of mitochondria yields submitochondrial particles (SMP) that contain ATP synthase capable of catalyzing ATP synthesis from medium ADP and P_i; the enzyme can also hydrolyze ATP when decoupled from the electrochemical energy. Studies of the ATP synthase on SMP revealed two physiologically separate components of the synthase: a solubilizable F_1 factor and a membrane embedded F_O factor; ATP synthase is thus also commonly referred to as the F_1F_O complex. F_1 contains the catalytic core of the complex while F_O serves to anchor F_1 to the membrane as well as channeling protons across the membrane.

The catalytic mechanism of ATP synthase, as well as its structure, is very complex. The enzyme is made up of five different subunits, namely α, β, γ, δ and ε, in the order of decreasing molecular weights (55, 50, 30, 20 and 15 kDa), with a stoichiomery of $\alpha 3\beta 3\gamma\delta\varepsilon$ (Figure 1). Based on the amino acid sequences of these polypeptides reported by Walker et al., the molecular weight of F_1 was determined to be 371,000 Da (4, 5). The use of monoclonal antibodies for the subunits of F_1 coupled with electron-microscopic techniques revealed the alternate arrangement of the α, β subunits in F_1 from E. coli and chloroplast (6, 7). The arrangement is asymmetrical, however, because there is contact with

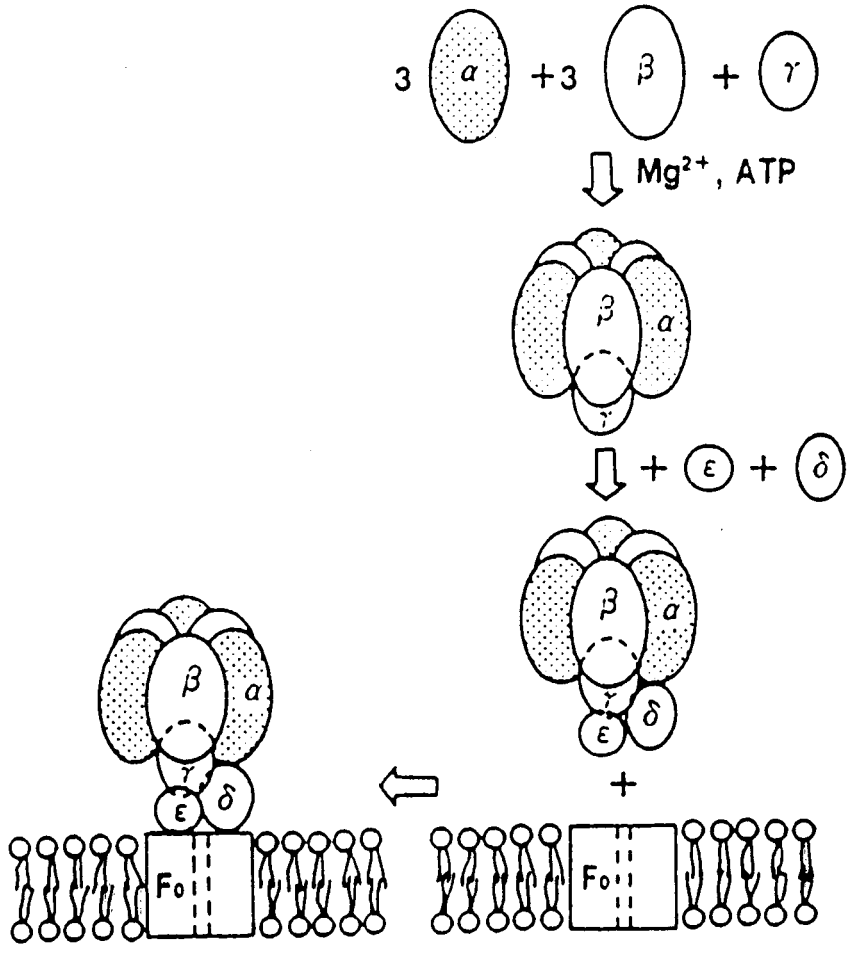

Figure 1
F_oF_1-ATPase

only a single copy of the γ, δ, and ε subunits. Interactions among the subunits in F_1 during enzyme catalysis is a major area of research. The subunit interaction is manifested in the mechanism of F_1 catalyzed ATP hydrolysis, namely negatively cooperative substrate binding and strong positive catalytic site cooperativity upon substrate binding.

The subunits of F_1 provide binding sites for six nucleotides (8, 9), three PP_i (10), and at least two P_i molecules (11, 12). The enzyme is associated with an inhibitor peptide (IP) that regulates its activity (13, 14); this peptide binds to β subunits (15) and is usually removed during purification of F_1.

The six nucleotide binding sites on F_1 have been probed mainly by studies of direct binding of the nucleotides and of nucleotide affinity analogs. The binding domains are located only on the α and β subunits, and possibly the interfaces between these two major peptides (review 2). Two types of binding sites have been characterized. Of the six nucleotide binding sites, three exchange the bound ligands with nucleotides in the medium so slowly that they are considered unlikely to be the sites of catalysis. These nonexchangeable sites, as they are called, are selective for an unmodified purine (adenine or guanidine) moiety of the nucleotide. On the other hand, the remaining three of the six binding sites place less stringent requirements on the type of nucleoside triphosphate which they accept. Nucleotides bound at these three sites exchange rapidly with nucleotides in the medium during catalytic turnover; they are thus referred to as the exchangeable sites. The three sites exhibit negative cooperativity of nucleotide binding (8, 9, 2). Cross et al. and some other workers assign these exchangeable sites as the catalytic sites of F_1 but this is not unaminously agreed upon. Other authors proposed

that these three sites are actually a single catalytic site with two regulatory sites (16), or possibly two alternating catalytic sites (17,18). The popular 'binding change mechanism' of F_1 presented by Cross and Boyer et al. is based on the concept of multicatalytic sites. This mechanism describes sequential involvement of two or three catalytic sites in the presence of excess substrate and explains the observed strong positive catalytic site cooperativity exhibited by F_1 in terms of the sharp decrease in affinity for the products upon binding of substrate at the other catalytic site (19, 20). Another important feature of this enzyme catalysis is the reversibility of ATP hydrolysis/synthesis under conditions of single site catalysis (low substrate concentration). This reversibility was convincingly shown in Boyer's lab using ^{18}O exchange measurements (20). The apparent equilibrium ratio of ATP/ADP is near unity and energy input is required for the release of synthesized ATP, rather than for covalent bond formation. F_1 hydrolyzes ATP under normal catalytic conditions but formation of tightly bound ATP by F_1 from medium ADP and Pi in dimethylsulfoxide medium (30% w/v) has been demonstrated (21).

In addition to the six nucleotide binding sites, F_1 also possesses three PP_i binding domains (10). One of the three sites is of high affinity with $K_d \sim 20\mu M$. Based on their studies, Issartel and coworkers suggested that PP_i and ADP share common binding domains on the β subunits. Two types of binding sites for P_i had been well characterized by Penefsky and Kasahara (11, 12). They identified one high affinity P_i binding site and the other nonsaturable, lower affinity site(s) present on the protein. In addition to the difference in affinities for P_i, the two types of P_i binding sites also deviate in their response to effectors and inhibitors of the ATPase. In their studies, Penefsky and Kasahara showed that the monoanionic P_i ($H_2PO_4^-$) is the form of the ligand

which binds to the enzyme at the high affinity site. At pH 7.5, K_d at this site is 80 μM (in terms of total P_i concentration).

Since the high affinity binding site for P_i represents a part of the active site, information on its topography and functional amino acid residues in its environment are important to the understanding of catalytic mechanism at molecular level. In a series of papers published by Vignais and his coworkers, they reported the use of the affinity label, 4-azido-2-nitrophenyl phosphate (ANPP) to explore the P_i binding sites on F_1-ATPases from mitochondria (22, 23, 24), E. coli (25) and chloroplasts (26). Upon photoinactivation, the analog labeled the β subunit of these proteins. In mitochondrial F_1, the amino acid residues labled were Ile-304, Gln-308 and Tyr-311. The same region was photolabeled by affinity analogs of adenine nucleotides (27), indicating this region as part of the catalytic site of F_1.

Besides ANPP, other useful probes for P_i binding sites include arsenate (As_i) and vanadate. The usefulness of vanadate as a photosensitizing agent to study enzymes was recently discovered by Gibbons and his colleaques (28, 29, 30). Upon irradiation with UV light at 260 nm or 365 nm, vanadate bound to dynein ATPase caused cleavage of the protein. This photocleavage also occurred with myosin ATPase and ribulose-1,5-bisphosphate carboxylase/oxygenase (31, 32, 33). An interesting finding by Yount et al. is that the photocleavage is at least a two step process in which cleavage is preceeded by modification of amino acid residue(s) at the vanadate binding site. In the case of myosin ATPase and carboxylase, the modification involved oxidation of serine residues. Photomodified enzymes had enhanced or inhibited activity but the change was reversible by reducing the oxidized

residues with reducing agents like $NaBH_4$. Vi is a structural analog of P_i, and has been used extensively as an inhibitor or activator in mechanistic studies of enzymes that catalyze formation or breaking of bonds to phosphate; its photosensitivity provides a new dimension to its application. There is great advantage in using Vi as a photoaffinity probe, the most obvious being its close structural similarity to P_i in contrast to other photoaffinity ligands such as ANPP, which differ considerably from the natural ligand.

Vanadate has been used to study ATPase of various types including dynein, myosin, proton-motive (e.g. F_1), and ion-translocating ATPases (e.g. Na^+-K^+ ATPase, Ca^{2+}-ATPase). Dynein, myosin and ion-motive ATPases show high sensitivity towards vanadate; they are inhibited by micromolar concentrations of vanadate (34, 35). F_1, on the other hand, is less sensitive to vanadate inhibition. Reported K_i value of vanadate for F_1 is 1.5 mM (36). The difference in sensitivity reflects basic differences in structure and catalytic mechanisms of these enzymes. The ion-motive ATPases catalyze ATP hydrolysis via formation of a phosphorylated enzyme intermediate, and they are inhibited upon vanadylation of the proteins. Dynein and myosin do not form phosphorylated intermediates, but binding of Vi and ADP to the enzymes forms a stable $E^*ADP^*Vi^*Mg^{2+}$ dead end complex (34, 35). In these two types of inhibition, the binding efficiency and inhibition are attributed to the ability of Vi to assume a pentacoordinate structure resembling the transition state for the reaction. Mitochondrial F_1, as well as proton-motive F_1-ATPase in chloroplasts, *E. coli*, and thermophilus bacteria, apparently have a catalytic mechanism which differs from that of myosin and dynein.

The chemistry of vanadium is very complex. It exists predominantly in three oxidation states of +3, +4 and +5 but the latter two forms are more commonly encountered. In aqueous solutions with pH above 3, vanadium(IV) is readily air-oxidized to vanadium(V). Various forms of vanadium(V) exist in solutions, including orthovanadate, divanadate, trivanadate, tetravanadate and oligomeric forms such as decavanadate. The distribution of the total vanadium atom concentration among these species is dependent on the pH, ionic strength, and total vanadium concentration present in the solution (37).

F_1 is inhibited by vanadium(V) and is relatively insensitive to vanadyl ions. However, it is not known which species of vanadium(V) is responsible for the inhibition. This assignment is essential for interpreting results from the study of interaction of vanadate with F_1. It was proposed in this project that such identification be established. In addition to the kinetic inhibition of F_1, vanadate was also used in this project as a sensitizing agent for photoinactivation of F_1.

OBJECTIVES

1 Characterize vanadate-sensitized photoinactivation of F_1 in terms of the dependence on length of exposure to UV at 365 nm and sensitizer concentration.

2. Examine the physical nature of photodamage incurred upon F_1.

3 Study the effect of ADP, PP_i and P_i on the vanadate-sensitized photoinactivation of F_1.

4. Study the inhibition of F_1-catalyzed ATP hydrolysis by vanadate and determine the pattern of inhibition.

5. Elucidate the identity of vanadate (V) species in solution responsible for the inhibition of F_1.

6. Determine the k_{obs} of dissociation of vanadate from F_1.

EXPERIMENTAL PROCEDURES

MATERIALS

All reagents used in these investigations were reagent grade, ACS, or enzyme grade quality. Common chemicals were obtained from usual sources. The following were obtained from Boehringer Mannheim: ATP (disodium salt), PEP (monopotassium salt), SOD (lyophilized, from bovine erythrocytes), BSA (lyophilyzed), HEPES, β-NADH (grade II), PK and LDH (from rabbit muscle) in ammonium sulfate suspension. Reagents and apparatus for electrolysis were obtained from Biorad except the ampholytes (pH 4-6.5 and pH 3-10) which were from Pharmacia. Sephadex G-50 (fine) was also from Pharmacia. Tris (Trizma Base), sucrose (grade I), ammonium sulfate and Triton X-100 were obtained from Sigma. Vanadium(V) oxide (99.999%, gold label) was from Aldrich. Monobasic potassium phosphate (KH_2PO_4) and dibasic potassium phosphate ($K_2HPO_4.3H_2O$) were from Anachem Co.. Pyrophosphate (sodium salt) was from BDH chemicals. The 1.0 mL tuberculin syringes for making centrifuge columns were purchased from Mandel Scientific Co.

METHODS

Preparation of Beef Heart Mitochondrial F_1-ATPase

F_1-ATPase was isolated from beef heart mitochondria using both heavy and light fractions of the mitochondria preparation by methods described by Knowles and Penefsky (39). The purified F_1 was stored at 4^o as an ammonium sulfate suspension until use.

Protein Determination

F_1 concentration was determined by the method of Lowry et al. (41) using BSA (ε_{280} = 0.667 $mL \cdot mg^{-1} \cdot cm^{-1}$) as standard. Concentration of other proteins was determined using either Biorad protein assay or Lowry method. For the (^{32}P)-phosphate binding study where F_1 was resuspended in Tris-OAc buffer, a modified Lowry procedure (42) was employed.

Sephadex Centrifuge Column Technique

Sephadex-G-50 (fine) was swollen overnight at 4^oC in 50 mM Tris-OAc pH 7.5 when the column was used for desalting coupling enzymes, or in F_1-buffer (0.15 M sucrose/2 mM $MgSO_4$/10 mM K^+-HEPES pH 8.0) when used for preparing F_1. Sephadex and buffer were mixed in the ratio of 5g : 100 mL. The emulsion was brought to room temperature before packing the column which was made from a 1.0 mL tuberculin syringe fitted with a porous polyethylene frit. The syringe was filled to the top with the swollen Sephadex and solution allowed to drip from the column. Excess solution retained in the columns was removed by centrifuging the columns in an I.E.C. tabletop centrifuge, swinging bucket rotor model 221, at 1050 x g (setting 5) for 1 min (2 min when

colums were used for F_1). The packed column had a volume of approximately 0.7 mL.

Desalting of Coupling Enzymes

Ammonium sulfate suspensions of PK and LDH were centrifuged at 27,000 x g, in a Sorvall RC-5B Centrifuge (15,000 rpm, 4-10^{o}C, 15 min, Sorvall SS-34 rotor). The pellet was resuspended in a small amount of Tris-OAc buffer. 100-125 µL aliquots were centrifuged through the packed columns (described in previous section) for 1 min in the I.E.C. tabletop centrifuge. The effluent was then pooled and diluted with cold Tris-OAc buffer to the appropriate concentration. The coupling enzymes were kept on ice during the experiment and excess enzyme stored at -70^{o}C.

Sephadex Column for Removing Unbound Ligands

The columns were prepared as described under the Sephadex centrifuge column technique. In the study of effect of ADP on photoinactivation, the enzyme had a concentration below 1 mg/mL. BSA was added to the mixture making a BSA concentration of 10 mg/mL. Presence of such a carrier reduced retention of F_1 in the column (8). Activities of the enzyme in the control before and after passing through the columns were compared as a means of estimating the change in F_1 concentration.

Desalting of F_1

Ammonium sulfate suspension of F_1 was centrifuged at 17,000 x g (12,000 rpm, 4-10^{o}C, 15 min, Sorvall SS-34 rotor). The supernatant was carefully removed and the pellet washed three times with cold 2 mM ammonium sulfate

pH 8.0 before dissolving the pellet in F_1-buffer which had been equilibrated at room temperature. The enzyme with a concentration greater than 1 mg/mL was then centrifuged through a packed Sephadex column for 2 min. The effluent was diluted with F_1-buffer to the desired concentration. The enzyme at this stage had a [2,1] state (two nonexchangeable sites and one exchangeable site filled with adenine nucleotides) of nucleotide binding site occupancy (39) and could be used for preparing F_1[3,0] (three nonexchangeable sites filled and three exchangeable sites empty).

Preparation of F_1[3,0]

The method for preparation of F_1[3,0] from F_1[2,1] was adopted from that described by Cunningham and Cross (40). The steps are depicted in Scheme 1.

Desalted F_1[2,1]
+
1000x molar excess MgATP
⇓
+ 1000x molar excess MgGTP
⬇
collect eluate
⬇
collect eluate
⇓
F_1[3,0]

2 min incubation

30 sec incubation

10 min incubation

10 min incubation

⇓ filter through Sephadex column equilibrated with F_1-buffer

⬇ filter through Sephadex column equilibrated with F_1-buffer containing 50 mM P_i, pH 7.0

Scheme 1

Preparation of F_1[3,0] from F_1[2,1]

During preparation, enzyme concentration was maintained above 1 mg/mL to minimize loss of the protein during centrifugation (8). The eluate collected from the last column was diluted with F_1-buffer and kept at room temperature throughout the experiment. Although F_1 is cold labile, the enzyme could be stored in liquid nitrogen. This was achieved by dropping 100-200 μL aliquots of the resuspended enzyme directly into a bath of liquid nitrogen. A pellet was formed instantaneously. Pellets formed were collected in polyethylene tubes and stored in a liquid nitrogen tank. When required, pellets of the frozen enzyme were thawed in a water bath at room temperature. Pellets of F_1 prepared in the same batch had similar protein concentrations and variation of enzyme activities was within 5%.

ATP Hydrolysis Assay

The rate of ATP hydrolysis catalyzed by F_1 was monitored by coupling the production of ADP to the oxidation of NADH. PK and LDH coupled the reactions as depicted in Scheme 2. When high concentrations of vanadate were present, vanadate-catalyzed oxidation of NADH was prevented with the addition of SOD. The assays were performed at 30°C in 1.5 mL assay mixtures at pH 7.5. The rate of oxidation of NADH was monitored at 340 nm (ε_{340} = 6.22 $mM^{-1} \cdot cm^{-1}$) with an HP 8452A Diode Array Spectrophotometer. One to six assays could be performed simultaneously. The highest linear rate at steady state was determined by the program in the computer linked to the spectrophotometer. The program employed an algorithm which detected a linear segment of the timedata (absorbance of the assay mixtures as a function of time) which had the steepest slope and must be comprised of at least 12 absorbance measurements taken during the assay. A criterion for the validity of the rate determination

was that when this segment was divided into four subsegments, the slope for each subsegment should be the same.

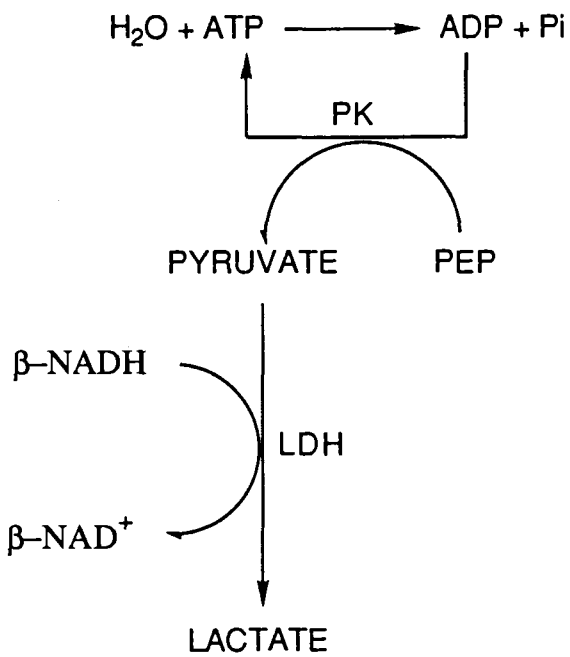

Scheme 2

ATP hydrolysis coupled with enzyme assay system

UV Irradiation of F_1

Irradiation was routinely performed with an 8 watt UV lamp from The Southern New England Ultraviolet Co. The irradiation spectrum spanned from 320 nm to 400 nm with maximum output at 365 nm. Enzyme mixtures were kept in microcapillary tubes made of bromosilicate glass and placed on glass plates mounted above the UV lamp. The glass plates sandwitched a layer of water that reduced transmittance of heat from the lamp to the enzyme samples. The samples were 2 cm away from the light source.

UV Irradiation of F_1 in Deoxygenated Medium

F_1 was desalted and resuspended in 100 μL F_1-buffer. Deoxygenated buffer was prepared by repeating freezing, vaccuming and thawing the solution three times under a nitrogen line. F_1 was diluted with this buffer to approximately 0.4 mg/mL. Eight samples were made following the procedure described in Scheme 3.

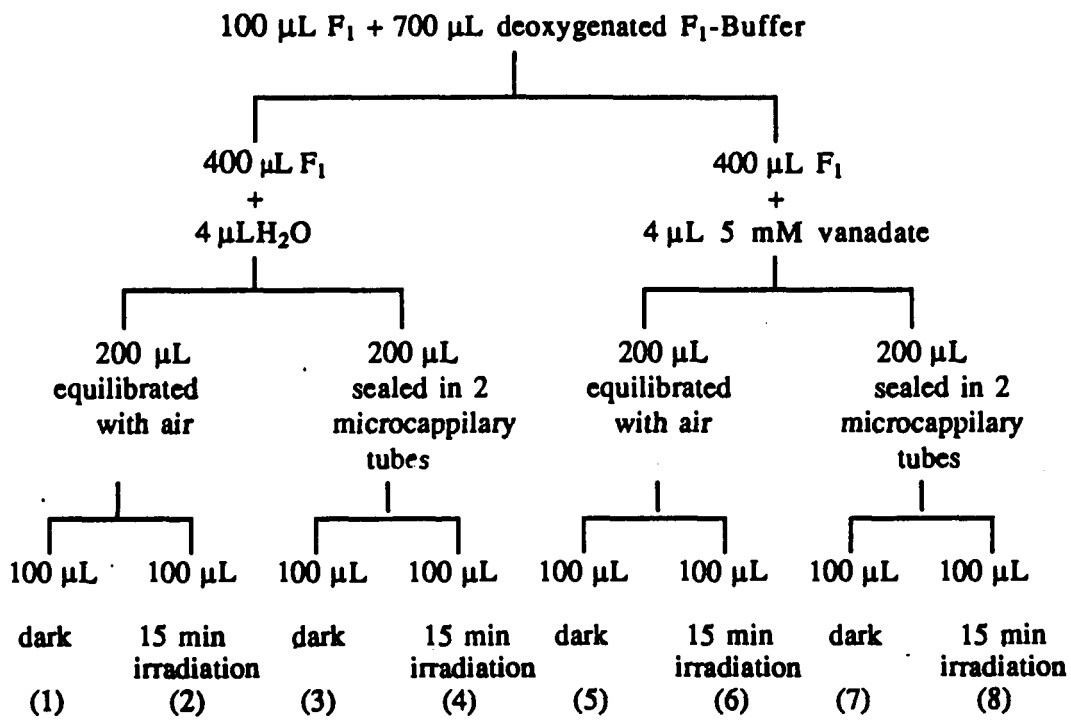

Scheme 3

Preparation of samples for study of vanadate-sensitized photoinactivation of F_1 under anaerobic condition.

Ten μL of each sample was used for activity assay in reaction mixture containing 50 mM Tris-OAc, 4.3 mM $MgCl_2$, 3 mM K^+-PEP, 0.21 mM NADH, 100 μg

PK, 80 μg LDH and 1 mM ATP. Vanadate solution and H_2O added to the enzymes were not deoxygenated prior to the addition.

SDS Polyacrylamide Gel Electrophoresis

Gels were made as described by Laemmili (43) with 2% stacking gel and 15% separation gel, using a Biorad mini-2D gel electrophoresis apparatus unless specified otherwise. The running current was 25 mA per plate in the stacking gel and 37.5 mA per plate in the lower gel. Fairbanks stain (0.05% Coomassie blue/25% isopropanol/10% acetic acid) was used for staining the gels while 10% acetic acid was used for the destaining.

Isoelectric Focusing Gel Electrophoresis

For isoelectric focusing of protein within a pH 4-6.5 gradient, the gel preparation and running conditions followed the methods described by O'Farrell (44). Nonequilibrium pH gradient electrophoresis (NEPHGE) was adopted for focusing protein within a pH 3-10 gradient (45). After staining with the Fairbank stain and before destaining with 10% acetic acid, the gels was treated with de-ampholine solution (25% isopropanol/10% acetic acid) until most of the background stain was removed.

Two-dimensional Gel Electrophoresis

2-D gel electrophoresis involved isoelectric focusing of the protein in the first dimension (pH gradient 3-10, using NEPHGE) followed by SDS-PAGE in the second dimension. F_1 was applied to the gel in the second dimension to provide standards for identification of the subunits resolved in the 2-D gel.

Protein sequencing

The peptides on SDS gel was electrotransferred to a PVDF microporous membrane and sent to Clinical Research Institute in Montreal for sequencing of the P_1 peptide.

^{32}Phosphate Binding Assay

Aliquots of 80 µL of F_1 suspended in 50 mM Tris, 2 mM $MgSO_4$ pH 7.5 was incubated 68 min at 20°C with various amounts of vanadate and 50 µM or 75 µM $^{32}P[P_i]$. The mixtures were filtered through Sephadex columns to remove unbound ligands. Column effluents were collected directly into polyethylene liquid-scintillation vials to which 0.5 mL water was added. Each sample was counted (Cerenkov radiation) for 5 min before transferring to test tubes for protein assay using modified Lowry procedure. The vials were washed thoroughly twice with 0.25 mL aliquots of water and pooled with previous solution.

Statistics

BMDP (Biomedical Computer Program) was used for nonlinear regression analysis.

^{51}V NMR for determination of vanadate species in assay mixture

^{51}V NMR spectra were obtained at 105 MHz with a Bruker WM-400 NMR spectrophotometer operating at ambient temperature. The pulse width was 50° with sweep widths of 40 kHz, and 0.05 s acquisition times. Integration of peak areas was performed with use of the instrument manufacturer's software. A line-broadening of 40 Hz was applied to all spectra before Fourier

transforming to the frequency domain with use of a 2K data set zero-filled to 8K. The formation constants of V_2 and V_4 were defined as:

$$2\,Vi \rightleftharpoons V_2 \qquad K_2 = \frac{[V_2]}{[Vi]^2}$$

$$4\,Vi \rightleftharpoons V_4 \qquad K_4 = \frac{[V_4]}{[Vi]^4}$$

RESULTS

(A) Photoinactivation of F_1 in presence of vanadate

F_1 incubated with vanadate lost its ATPase activity upon exposure to UV light at 365 nm. Irradiation of F_1 alone at this wavelength did not have a detrimental effect on the enzyme activity unless the exposure time was prolonged beyond 30 minutes (Figure 2). F_1 incubated with P_i did not undergo photoinactivation; the presence of vanadate was therefore essential for the sensitized photoinactivation of F_1 to take place. The rate of photoinactivation on a semi-log scale was nonlinear, the enzyme had lower sensitivity to light after 30 minutes exposure (Figure 3). Vanadate-sensitized photoinactivation of F_1 therefore did not appear to be a first order reaction.

Photoinactivation of F_1 was an all or none effect. The irradiation changed the population of active enzyme but not the catalytic properties of it. This can be seen from the reciprocal plot of the enzyme activity in Figure 4. V_{max} of the photoinactivated enzyme (F_1 + 250 μM vanadate irradiated for 30 minutes) was lower than that of the controls but it retained the same K_m for ATP. It should be mentioned that F_1 lost activity during the experiment; however, vanadate added to F_1 and kept in the dark stabilized the enzyme activity. As a result, the activity of the F_1 control (not exposed to light) was lower than that of the F_1 + vanadate control after 60 minutes incubation (□ and ● in Figure 4).

Figure 2. **Time-dependence of vanadate-sensitized photo-inactivation of F_1.**

F_1 at 0.3 mg/mL suspended in F_1-buffer was incubated in the dark with 100 μM P_i (◇) or 100 μM vanadate (○) for 30 minutes. No P_i or vanadate was added to the control (□). At the end of 30 minute incubation, aliquots of the mixture in microcapillary tubes were exposed to UV irradiation for the length of time as shown. Enzyme aliquots of 5 μL were used for activity assays in assay mixtures containing 4.3 mM $MgCl_2$, 2 mM K^+-PEP, 0.21 mM NADH, 50 μg PK, 40 μg LDH, 1 mM ATP in 50 mM Tris-OAC buffer of pH 7.5. Remaining activity was determined as the ratio of activities of enzyme exposed to UV irradiation and enzyme that was kept in the dark at ambient temperature (20^o).

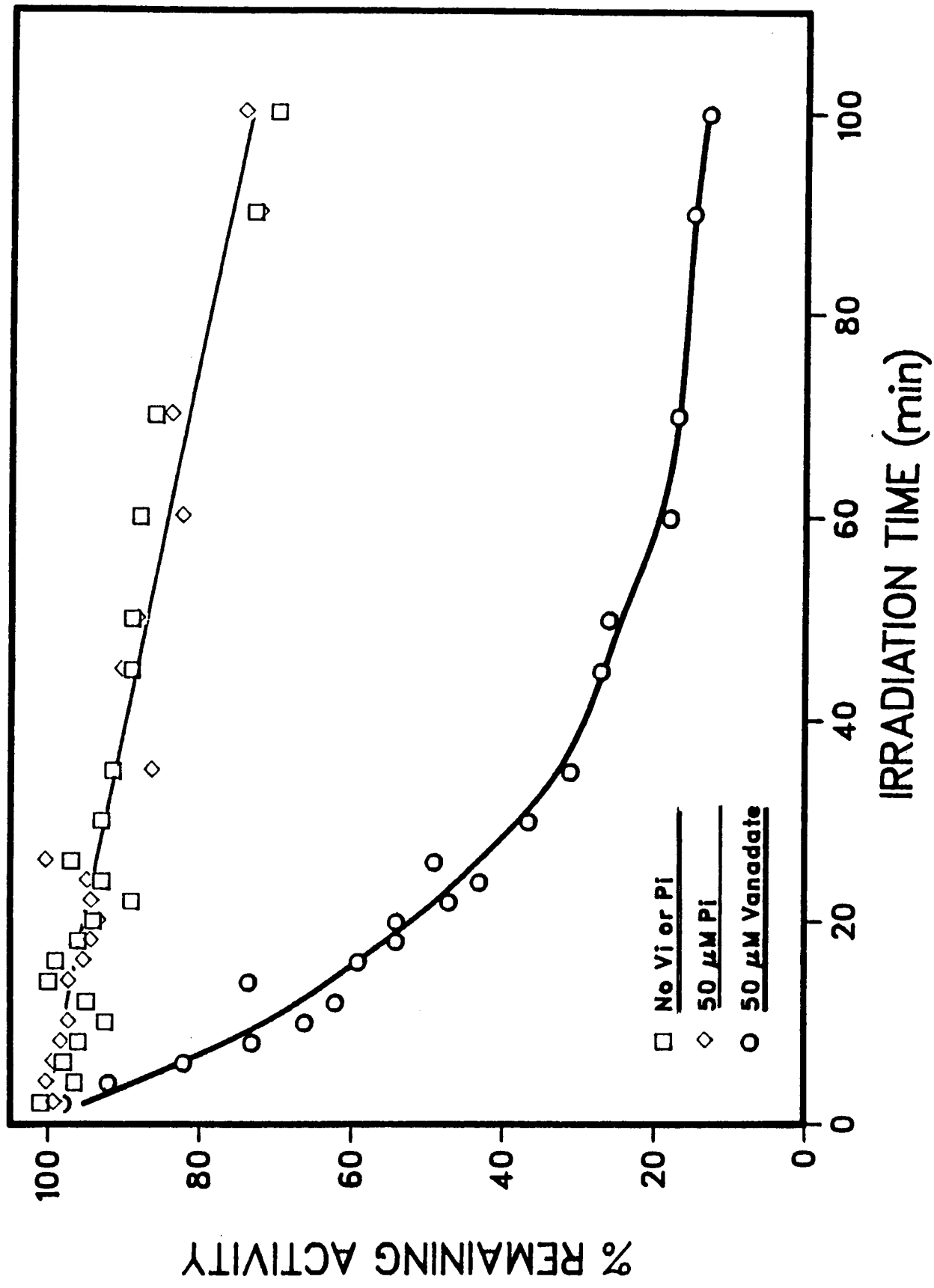
% REMAINING ACTIVITY
100
80
60
40
20
0
0
20
40
60
80
100
IRRADIATION TIME (min)
No Vi or Pi
50 μM Pi
50 μM Vanadate

Figure 3. **Semi-log plot of Figure 2.**

Data showing remaining activities of F_1 incubated with 50 μM vanadate after exposing to UV irradiation.

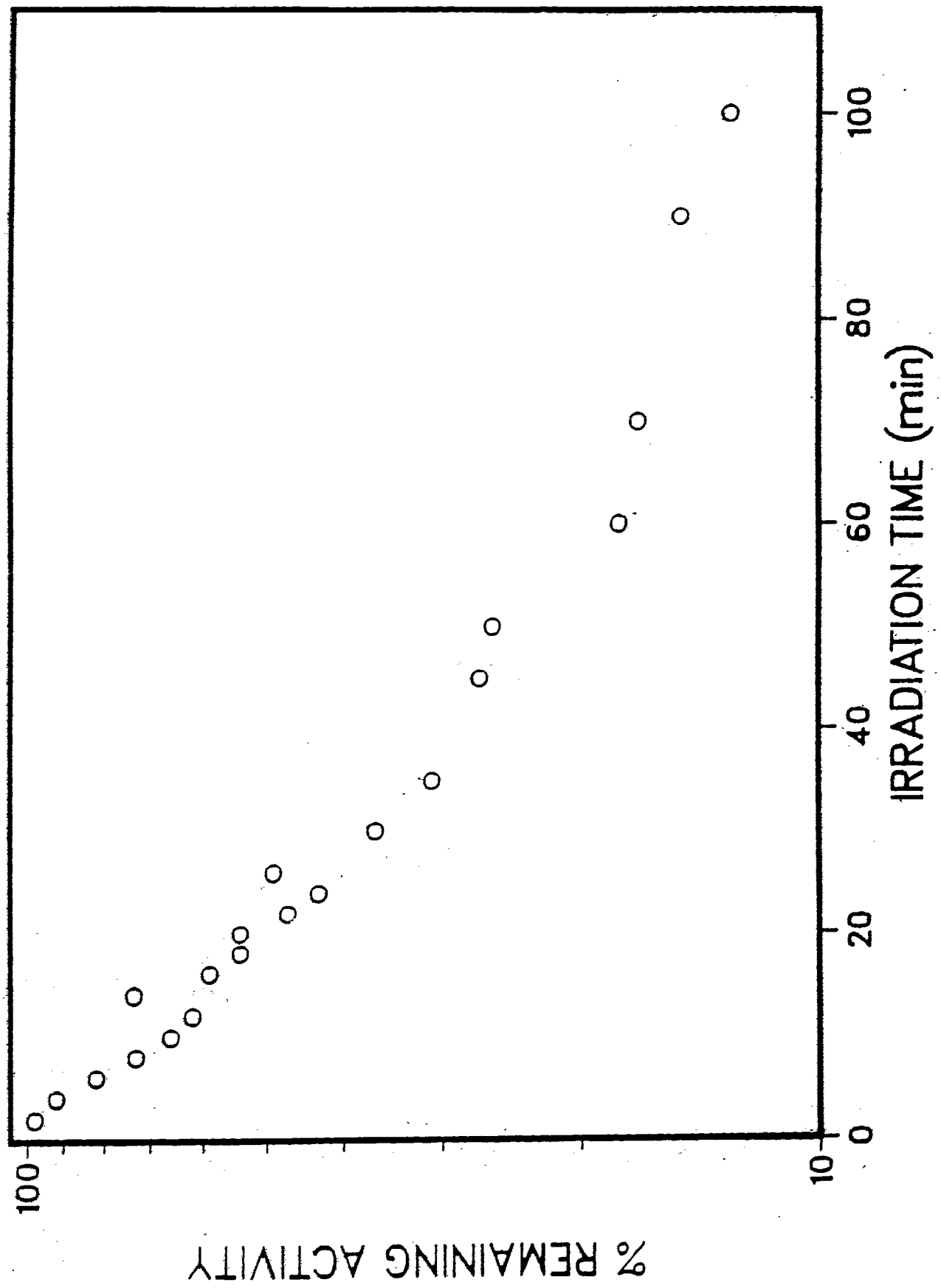
% REMAINING ACTIVITY
100
10
0
20
40
60
80
100
IRRADIATION TIME (min)

Figure 4. **Double reciprocal plot of activity of photoinactivated F_1.**

F_1 of 0.13 mg/mL was incubated with or without 250 μM vanadate for 60 minutes before exposing to 30 minute UV irradiation. Corresponding controls were kept in the dark at ambient temperature. For the two samples incubated with vanadate, vanadate was not removed from the incubation mixture before the activity assay. The final vanadate concentration in the assay mixture was 1.7 μM. The assay solution contained 2.14 mM $MgCl_2$, 3 mM K^+-PEP, 0.21 mM NADH, 50 μg PK, 40 μg LDH and various amounts of MgATP as shown in the figure. The mixture was maintained at pH 7.5 with 50 mM Tris-OAc. 1.3 μg F_1 was added to initiate the reaction. From the graph, K_m was determined to be 0.071 mM.

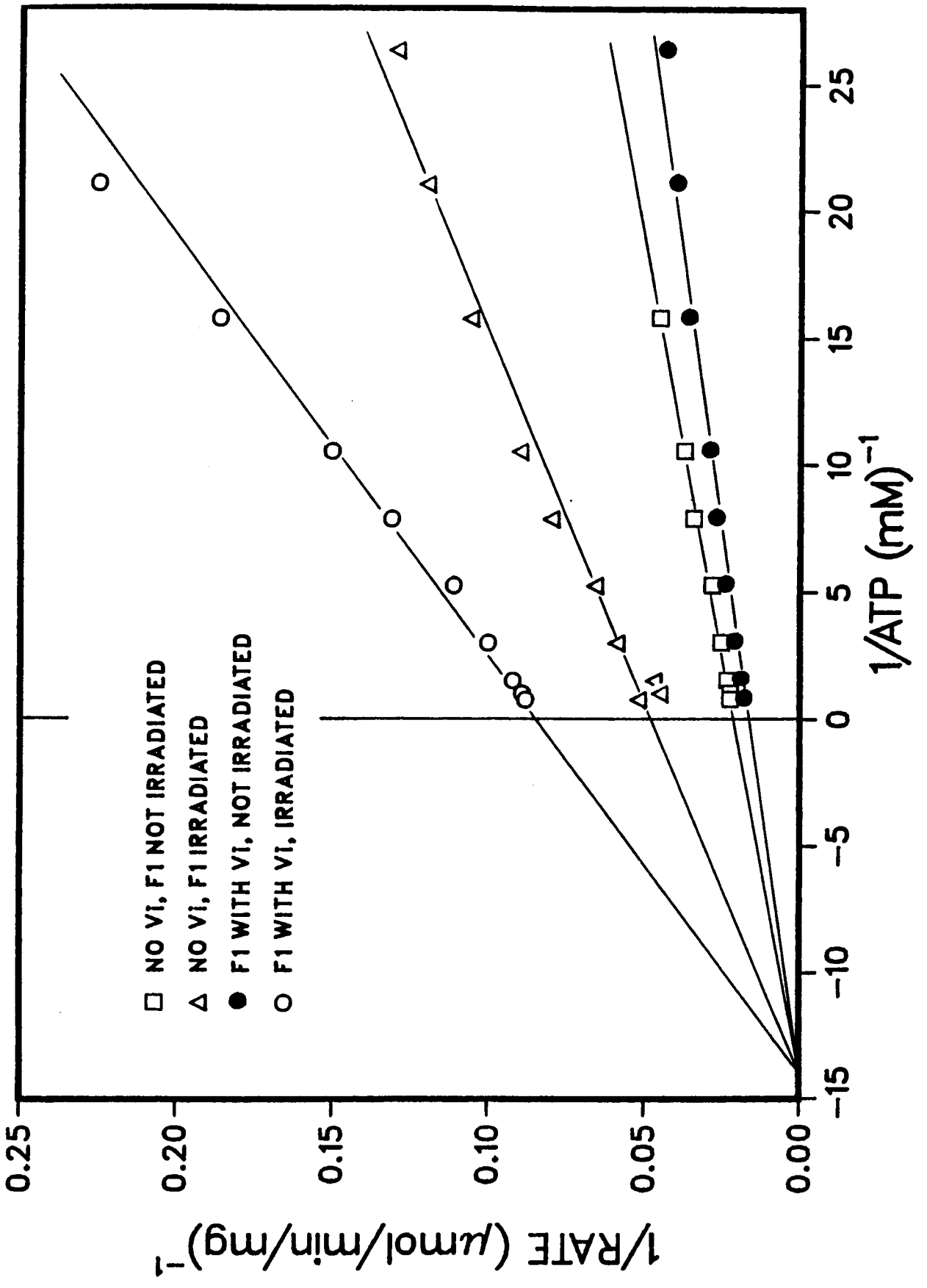
0.25
0.20
0.15
0.10
0.05
0.00
1/RATE (μmol/min/mg)⁻¹
−15
−10
−5
0
5
10
15
20
25
1/ATP (mM)⁻¹
□ NO Vi, F1 NOT IRRADIATED
△ NO Vi, F1 IRRADIATED
● F1 WITH Vi, NOT IRRADIATED
○ F1 WITH Vi, IRRADIATED

In addition to the length of irradiation time, the extent of photoinactivation was a function of the amount of vanadate incubated with F_1. Figure 5 shows such concentration dependence when all the samples were irradiated for 45 minutes. The graph shows maximum photoinactivation at [vanadate] > 200 μM. However, the inactivation was not 100% complete within the vanadate concentration range used in the experiment. In the reciprocal plot (Figure 5B) derived from Figure 5A, the y-axis was expressed as the reciprocal of (0.95-Remaining Activity) since the enzyme with no vanadate added lost 5% activity after the irradiation. A straight line was obtained in Figure 5B. A similar graph was produced when the total vanadium concentration was replaced with corresponding monovanadate concentration on the horizontal axis in Figure 5C. The linear relationship between the inverse of the remaining activity and monovanadate concentration indicates that monovanadate was the form of vanadate interacting with the enzyme during the process of photoinactivation. The observed K_i for such interaction determined from Figure 5C is 12.3 $\pm$ 0.9 μM Vi.

The physical changes in the protein upon UV irradiation in the presence of vanadate were studied using gel electrophoresis. When the treated enzyme was run on the SDS-PAGE, new peptides appeared on the gel (Figure 6). UV light of 365 nm and presence of vanadate appeared to cause photocleavage of F_1. The cleaved peptide was one of the heavy subunits (α or β) since one of the new bands ran behind other three lighter subunits of F_1. Another new band was lighter than the γ subunit

Figure 5. **Vanadate concentration dependence of photoinactivation of F_1.**

Approximately 0.3 mg/mL F_1 suspended in F_1-buffer was incubated with the indicated concentrations of vanadate for 30 minutes before exposing to 45 minutes of UV irradiation. 5 μL of the enzyme was used in the activity assay. The assay mixture contained 4.3 mM $MgCl_2$, 2.67 mM K^+-PEP, 0.21 mM NADH, 60 μg PK, 45 μg LDH, and 1 mM ATP buffered at pH 7.5 with 50 mM Tris-OAc. The remaining activity was calculated as the ratio of activities of enzyme exposed to irradiation to that of the enzyme incubated with the same amount of vanadate but kept in the dark. The enzyme with no added vanadate had an activity of 0.136 AU/min before irradiation and 0.13 AU/min after receiving 45 minutes UV irradiation. Graph (A) shows the remaining activities of all the samples with the indicated total amount of vanadate incubated with the enzyme. Graphs (B) and (C) are the reciprocal plots for (A) with the x-axis representing the reciprocal of total vanadium concentration (B) or monovanadate concentration (C). The formation constants used for the calculation of monovanadate concentration are K_2 = 0.21 mM^{-1} and K_4 = 0.37 mM^{-3}.

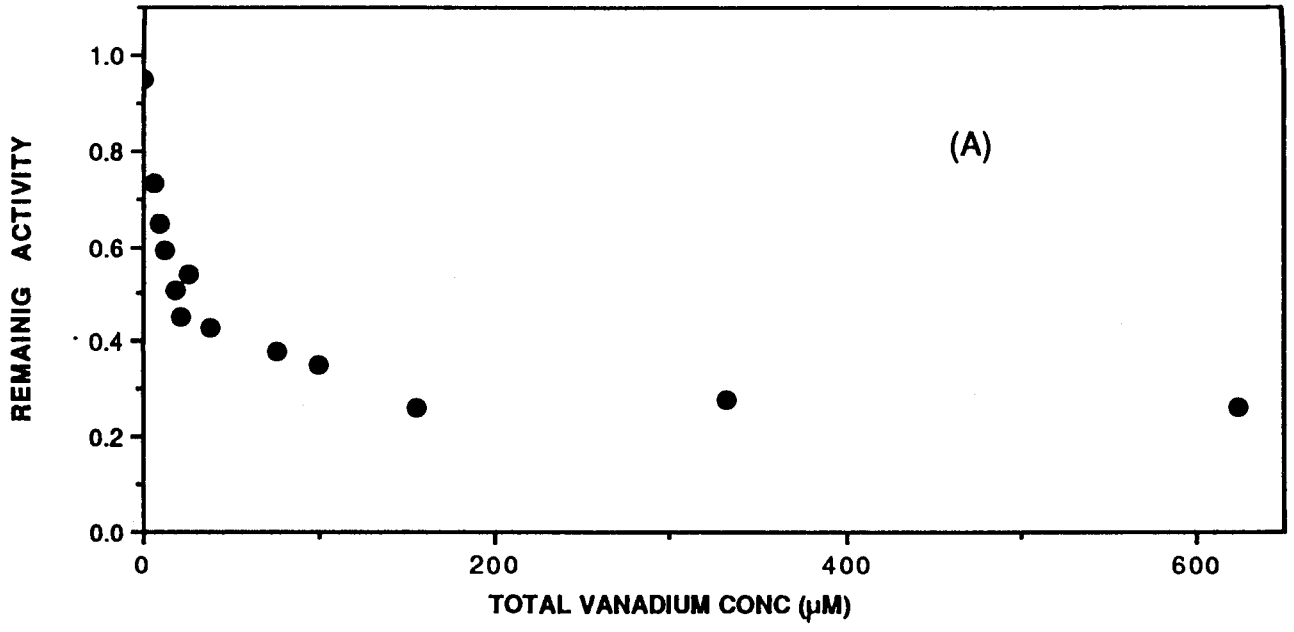
(A)
REMAINIG ACTIVITY
1.0
0.8
0.6
0.4
0.2
0.0
0
200
400
600
TOTAL VANADIUM CONC (μM)

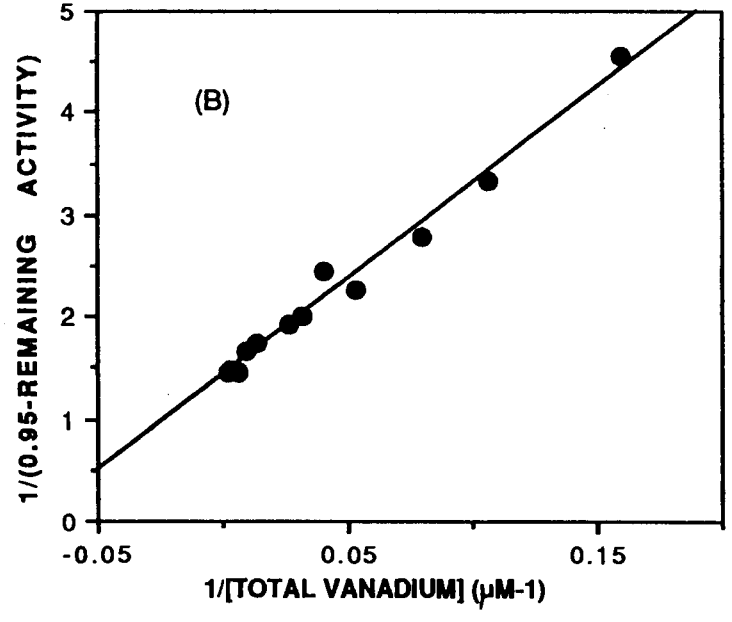
(B)
1/(0.95-REMAINING ACTIVITY)
5
4
3
2
1
0
-0.05
0.05
0.15
1/[TOTAL VANADIUM] (μM-1)

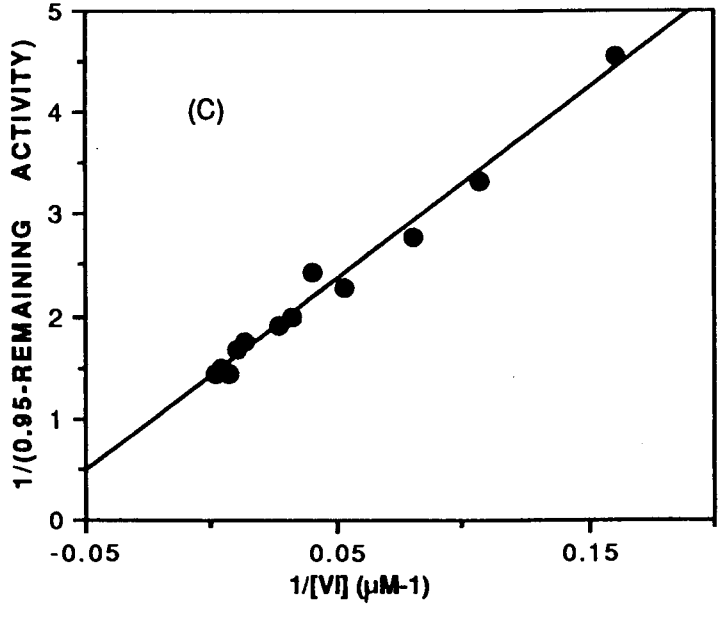
(C)
1/(0.95-REMAINING ACTIVITY)
5
4
3
2
1
0
-0.05
0.05
0.15
1/[VI] (μM-1)

Figure 6. **SDS-PAGE of photoinactivated F_1.**

Approximately 1 mg/mL F_1 in F_1-buffer with or without 250 μM vanadate was irradiated for the indicated length of time after a 30 minute incubation in the dark. Enzyme aliquots of 10 μL were run on the SDS polyacrylamide gel. The two gels shown were cast and run simultaneously.

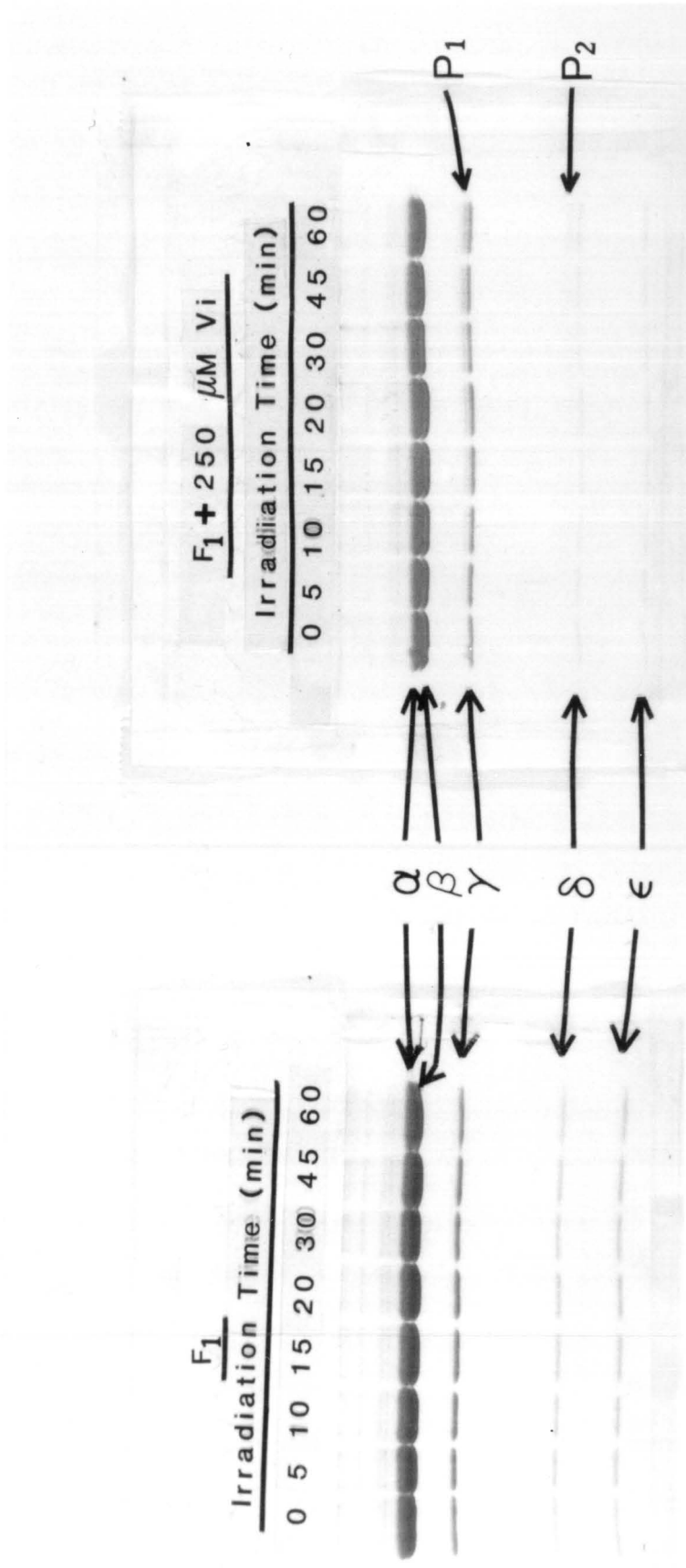
F1
Irradiation Time (min)
0 5 10 15 20 30 45 60
F1 + 250 μM Vi
Irradiation Time (min)
0 5 10 15 20 30 45 60
P1
P2
α
β
γ
δ
ε

but heavier than the δ and ε subunits. The two new bands which appeared on the gel will be referred to as P_1 and P_2 respectively. It is also possible that the P_1 and P_2 bands were modified γ and δ subunits with altered mobility on the SDS gel.

Although the treated enzyme had lost most of its activity (~20% remaining activity), the dye intensities of the heavy subunits, as well as the γ and δ bands , such as those seen in Figure 6 (F_1 + Vi gel, last lane), were still comparable with those of the controls. This may be due to the presence of inactive protein molecules in the original enzyme preparation which for some reason did not bind vanadate, or were not photocleavable (heavy subunits) or modifiable (γ and δ subunits) under the conditions of the experiment. For the α and β peptides, it is also possible that a form of modification other than peptide cleavage had caused the inactivation of F_1. The latter possibility was investigated by using gel electrophoresis. The control and the treated enzyme were analyzed on isoelectric focusing gels as shown in Figure 7. On an IEF pH 4-6.5 gradient gel, the photoinactivated enzyme (lanes 6, 9, 15, 18) had two extra bands compared with the controls (lanes 1, 2, 3, 4, 7, 10, 11, 12, 13 and 16). The bands on the IEF gel were identified according to their molecular weights and appeared on the two-dimensional gel shown in Figure 8. The peptides migrated in the pH 4-6.5 region and had M_r similar to the β subunits. Walker et al. also located β components in the acidic region and α components in the alkaline region of their 2-D gel (5). According to the results of amino acid sequencing of β subunits reported by Walker et al., β subunits of F_1 are heterogeneous with variable N-terminal residues. They obtained four partially resolved forms of β

subunit upon isoelectric focusing. On the gel displayed in Figure 7, three charged species of native F_1 were resolved. Two major bands are of equal intensities while the third band, having lowest pI among the three, was present in much lesser amount. The two new peptides, appearing after photoirradiation of F_1 in the presence of vanadate, showed different dye intensities. The fainter band, referred to as β'1, was focused in between the two major native β bands. The other band, referred to as β'2, fell below all the other bands on the IEF gel, and was in close proximity to the minor native β subunit. These peptides were not the products of photocleavage since they comigrated with the native β subunits on the second dimension SDS-PAGE; instead, they seemed to be modified β subunits that might be the intermediates in the photocleavage process. The occurrence of photomodification prior to photocleavage was shown by Yount et al. in their study of vanadate-sensitized photoinactivation of myosin ATPase (31, 32).

Although the modification and the possible occurrence of cleavage of the heavy subunits of F_1 resembled that of myosin ATPase, the photoinactivation of F_1, unlike that of myosin ATPase, could not be reversed by treating the photoinactivated enzyme with the reducing agent $NaBH_4$. The photoinactivated enzyme was not reactivated with the addition of dithiothreitol, cysteine or $NaBH_4$. Activity of the cleaved enzyme could not be recovered at all, but the possibility that reversal of the photomodification could be detected by the disappearance of β'1 or β'2 on the IEF gels was tested. F_1 incubated with 110 μM vanadate had 63%, 45%, and 35% remaining activity after 30, 60 and 90 min irradiation, respectively. Treating this photoinactivated enzyme with a 100x molar

Figure 7. **Isoelectric focusing of photoinactivated F_1**

Approximately 1.3 mg/mL F_1 was incubated 30 min with 50 mM vanadate and 50 mM P_i or with vanadate alone. The control and the samples were illuminated for 0, 2, 20 min. Aliquots of the mixture were loaded and run on the IEF gel with a pH gradient of 4-6.5. A gel size of 12 cm x 16 cm was used in the electrophoresis with a Biorad protein II cell.

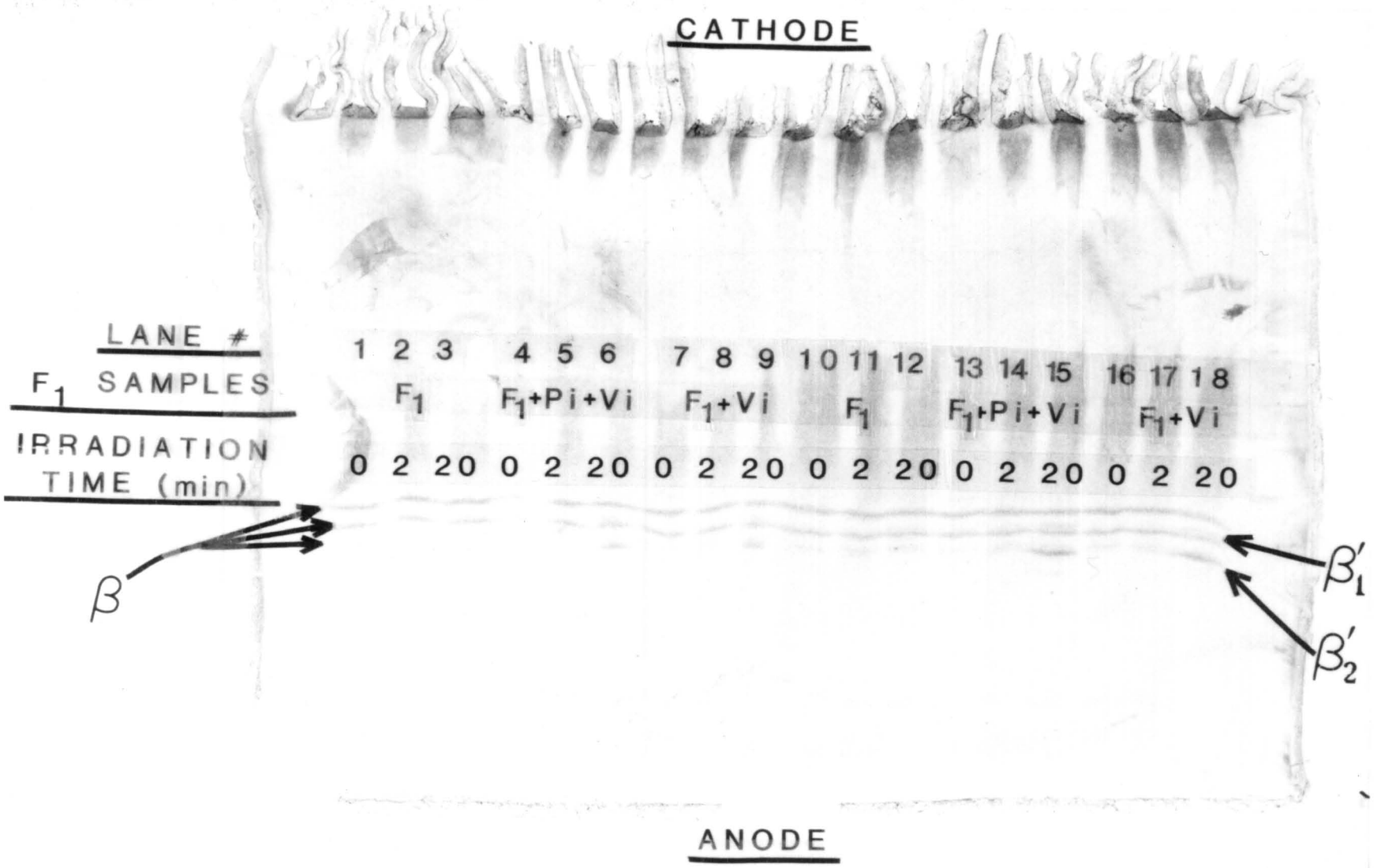
CATHODE
LANE #
1 2 3 4 5 6 7 8 9 10 11 12 13 14 15 16 17 18
F1 SAMPLES
F1 F1+Pi+Vi F1+Vi F1 F1+Pi+Vi F1+Vi
IRRADIATION TIME (min)
0 2 20 0 2 20 0 2 20 0 2 20 0 2 20 0 2 20
β
β'1
β'2
ANODE

Figure 8. **2-D gel electrophoresis of photoinactivated F_1.**

F_1 incubated with 50 μM vanadate was irradiated for 30 min with 41% remaining activity. Isoelectric focusing of 15 μg of the protein was carried out between pH 3 and 10. The second dimension was the SDS slab gel. The acidic end of the IEF gel was at the right hand side of the slab gel as shown. 10 μg untreated F_1 was run simultaneously on the gel in the second dimension and appeared on the right hand side of the gel.

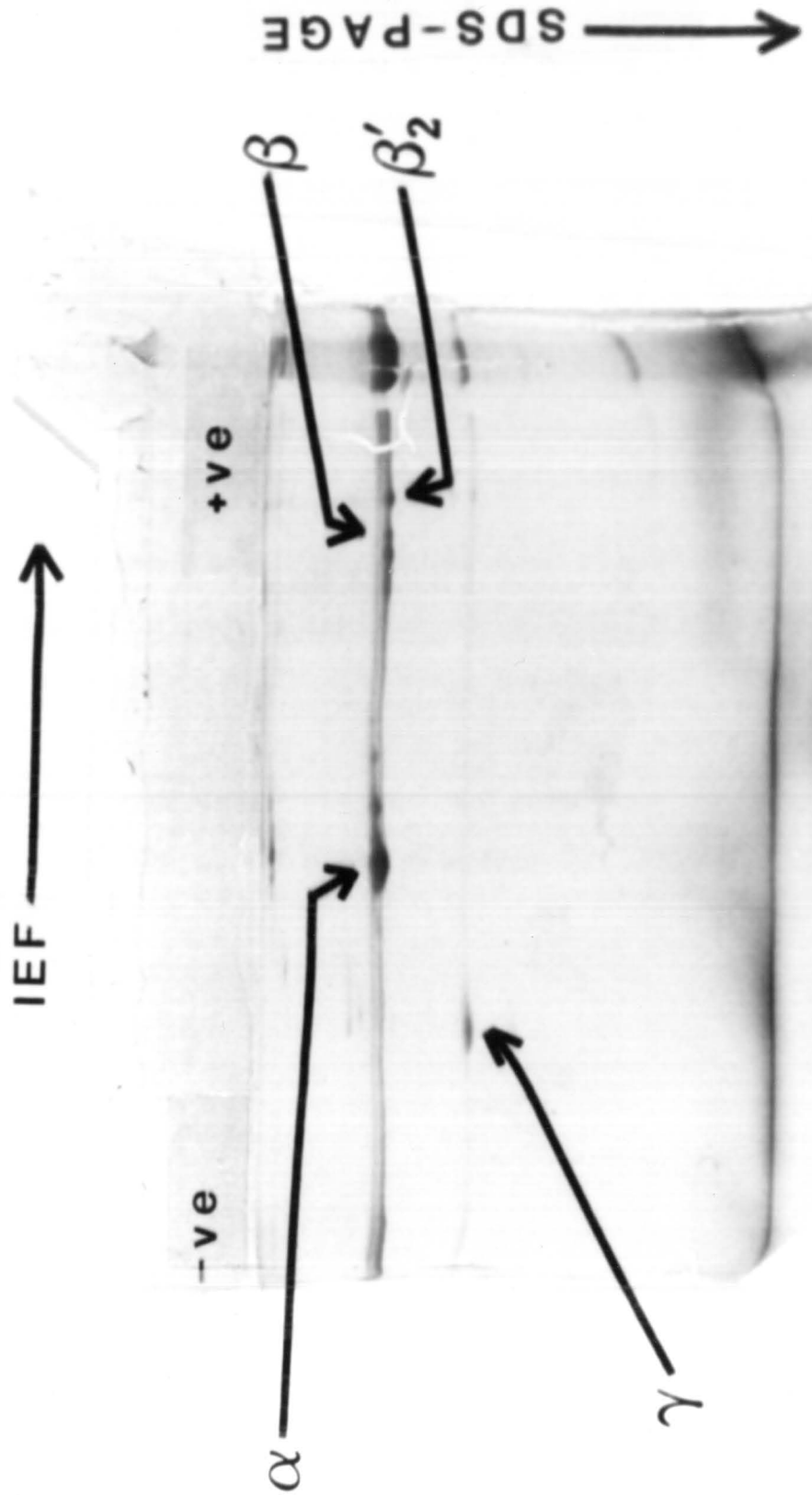
SDS-PAGE
IEF
+ve
-ve
β
β'2
α
γ

excess of $NaBH_4$ did not reactivate the enzyme. Isoelectric focusing of this treated F_1 on the mini gel (8 cm x 10 cm) disclosed only the β'2 band. The two major bands corresponding to the native β subunits were very close on the mini gel. β'1 was probably obscurred by these bands. Nonetheless, β'2 was recognizable on the gel and it did not disappear after treating the modified enzyme with $NaBH_4$. In another experiment, dithiothreitol and $NaBH_4$ were added to F_1 and vanadate preincubation mixture, but even the presence of these reducing agents in the mixture during photoirradiation had no observable effect on the photoinactivation process of F_1.

An attempt to identify the origin of the P_1 peptide was made. The subunits of the photoinactivated enzyme were separated by SDS-PAGE with prolonged running time to obtain better resolution of P_1 band and the γ subunit band. The separated peptides were then electrotransferred to a PVDF microporous membrane and subsequently submitted for sequencing. The cleaved products, although they appeared as two single bands on the electrophoretic gel, were found to be inhomogeneous. Amino acid sequencing of the P_1 peptide could not be conclusive because its N-terminal was ragged.

(B) Effects of P_i, PP_i, and ADP on photoinactivation

P_i, PP_i and ADP are ligands that have specific binding sites on F_1. The effects of these ligands on the vanadate-sensitized photoinactivation of the enzyme were studied to give insights into the nature of vanadate binding site(s) on F_1. Both PP_i and ADP have an inhibitory effect on P_i binding (10, 11). The influence of these species on photoinactivation is of particular interest since the interaction of Vi, a structural analog of P_i, with F_1 can be compared with that of P_i.

Binding of ATP, AMPPNP or ADP to F_1 causes release of P_i bound on the protein (46). Since bound ADP inhibits the enzyme, and since kinetic activity was the parameter monitored to assess the degree of photoinactivation, ADP had to be removed prior to the activity assay. This was done by filtering the enzyme incubated with vanadate and ADP through a Sephadex centrifuge column. In the centrifugation control (triplicates) where no ligand was added to F_1, the activity of the enzyme was 80-85% that of the enzyme before the centrifugation. A small amount of protein was retained in the columns. However, since all irradiated samples and their respective controls (with same amount of ligand but not irradiated) underwent the centrifugation process, the loss in protein was assumed to be equal. This is justified by the fact that the three centrifugation controls had lost comparable amount of F_1 in the filtering process. The activities of all enzyme samples after removing unbound ligands were thus not corrected for this discrepancy. The results from experiments designed to assess the effect of the presence of ADP on the photoinactivation are tabulated in Table I. Remaining activities of F_1 were

higher when ADP was added to the incubation mixture. The amount of protection against photoinactivation was proportional to the ADP concentration present.

Table I

Effect of presence of ADP on vanadate-sensitized photoinactivation of F_1

[ADP] in incubation mixture	% Remaining F_1-ATPase activity
none	22
0.05 mM	25
0.10 mM	28
0.50 mM	64
1.0 mM	61

F_1 at 0.3 mg/mL suspended in F_1-buffer was incubated with 50 μM vanadate and the indicated amount of ADP for 30 min before exposure to 15 min UV irradiation. ADP and vanadate were removed from F_1 prior to activity assay by centrifugation through a Sephadex column equilibrated with F_1 buffer. Effluent aliquots of 5 μL were used to initiate ATP hydrolysis in assay mixtures containing 50 mM Tris-OAc, 4.3 mM $MgCl_2$, 2.3 mM K^+-PEP, 0.21 mM NADH, 50 μg PK, 40 μg LDH, and 1 mM ATP at pH 7.5. Remaining activity was determined as the ratio of the activity of enzyme exposed to irradiation to the activity of enzyme containing the same amount of vanadate and ATP but which had been shielded from exposure to light.

PP_i has a dual effect on P_i binding to F_1. Issartel and his colleaques reported that at a concentration lower than 100 μM, the ligand enhanced association of P_i with F_1; at higher concentration the reverse effect was observed (10). The PP_i effect on the vanadate-sensitized photoinactivation

was therefore investigated over a wide concentration range and the result is depicted in Figure 9. PP_i at concentrations below 120 μM enhanced photoinactivation, while at higher concentrations it protected the enzyme from photoinactivation. The degree of protection also depended on the amount of PP_i added. In the presence of 10 mM PP_i, F_1 was no longer susceptible to photoinactivation. This phenomenon is comparable to the interference of P_i binding on F_1 by PP_i reported by Vignais et al (10). At low PP_i concentrations, PP_i increases P_i binding on F_1, but PP_i at higher concentrations inhibits the P_i from binding to the enzyme. The results therefore support the hypothesis that vanadate occupies the P_i binding site on the protein.

Unlike PP_i and ADP, P_i provided little protection of F_1 against photoinactivation (Figure 10). It was expected that if vanadate binds to F_1 as a P_i analog, then their binding should be competitive. The negative result shown in Figure 10, however, does not rule out the possibility that vanadate can bind to the P_i binding site. The reason is that it had been established from the study of inhibition of P_i binding to F_1 by vanadate that the two molecules can bind to the enzyme simultaneously (47 and Figure 11). The model for such simultaneous binding was proposed by Bramhall (47) and is shown in Figure 12. The constants obtained by fitting equation (A) (Appendix 1) derived for the model to the experimental data are listed along with the model. The solid line in Figure 11 represents the fitted curve; deviation of the experimental data from the calculated curve is fairly small. It is noteworthy that the K_V determined from the model is similar to the observed K_i of 12.3 $\pm$ 0.9 μM Vi calculated from the vanadate concentration dependence of photoinactivation of F_1 (Figure 5C).

Figure 9. **Effect of presence of PP_i on the vanadate-sensitized photoinactivation of F_1.**

F_1 at a concentration of approximately 0.6 mg/mL was incubated without PP_i or vanadate (Δ), or with 50 μM vanadate and the indicated amount of PP_i (O) for 30 min before exposure to 60 min irradiation. Activity was determined using 5 μL aliquots of the resulting enzyme mixture in an assay solution containing 4.3 mM $MgCl_2$, 2.67 mM K^+-PEP, 0.21 mM NADH, 60 μg LDH, 75 μg PK and 2 mM MgATP in 50 mM Tris-OAc buffer at pH 7.5. PP_i and vanadate were not removed form the incubation mixture prior to activity assay. Remaining activity was determined as the ratio of activities of the enzyme exposed to irradiation to that of the enzyme incubated with same amount of vanadate and PP_i but not exposed to UV irradiation.

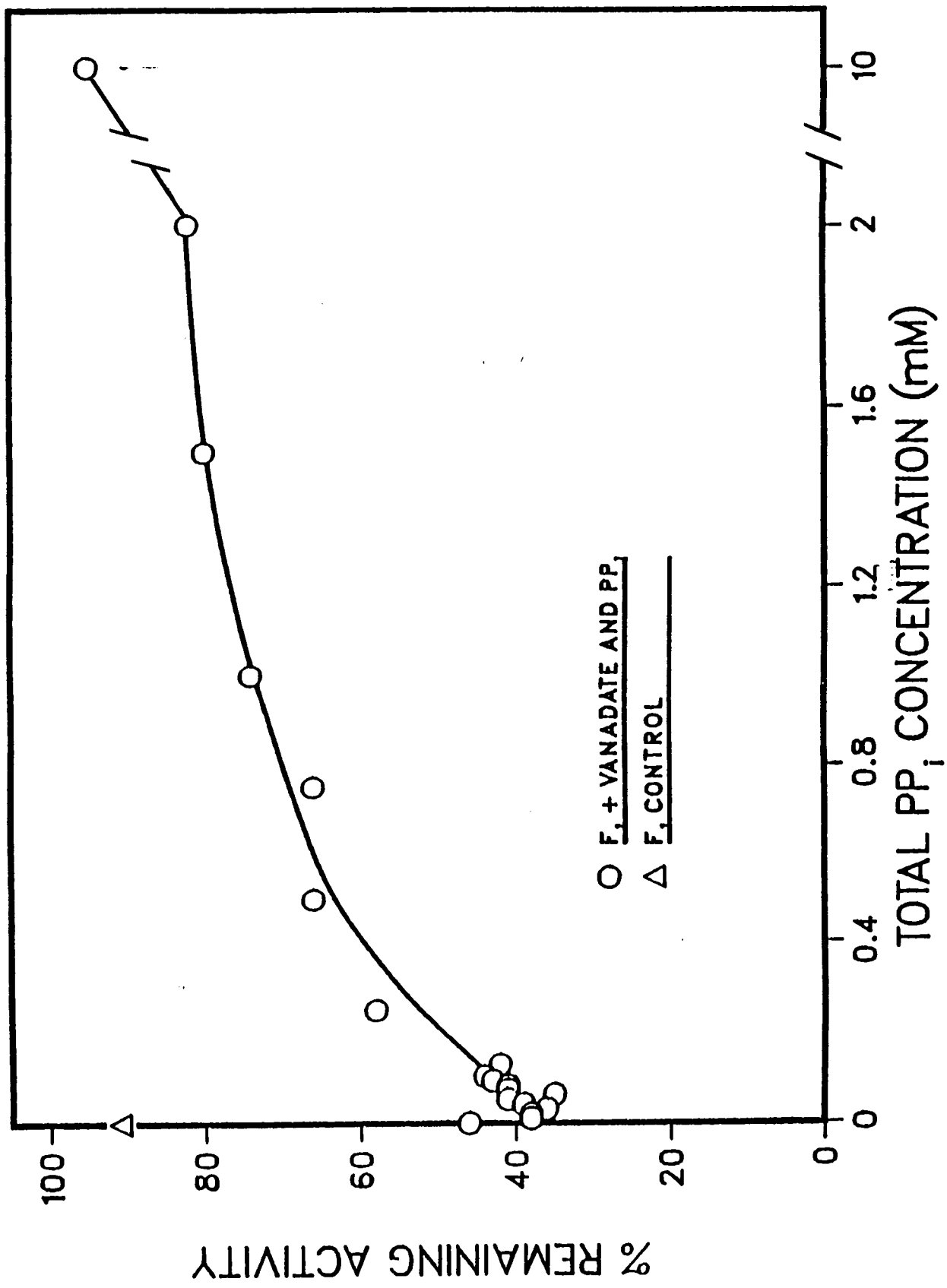
% REMAINING ACTIVITY
100
80
60
40
20
0
0
0.4
0.8
1.2
1.6
2
10
TOTAL PP$_i$ CONCENTRATION (mM)
O F_1 + VANADATE AND PP$_i$
Δ F_1 CONTROL

Figure 10. **Effect of presence of P_i on the vanadate-sensitized photoinactivation of F_1.**

F_1 was incubated without vanadate or P_i (Δ), or with 40 μM vanadate and the indicated amounts of P_i (O) for 30 minutes before exposure to 60 minute irradiation. Enzyme assays were carried out using 5 μL aliquots of enzyme in assay system described in the legend to Figure 10 but containing 1 mM MgATP. P_i and vanadate were not removed from the incubation mixture prior to activity assay.

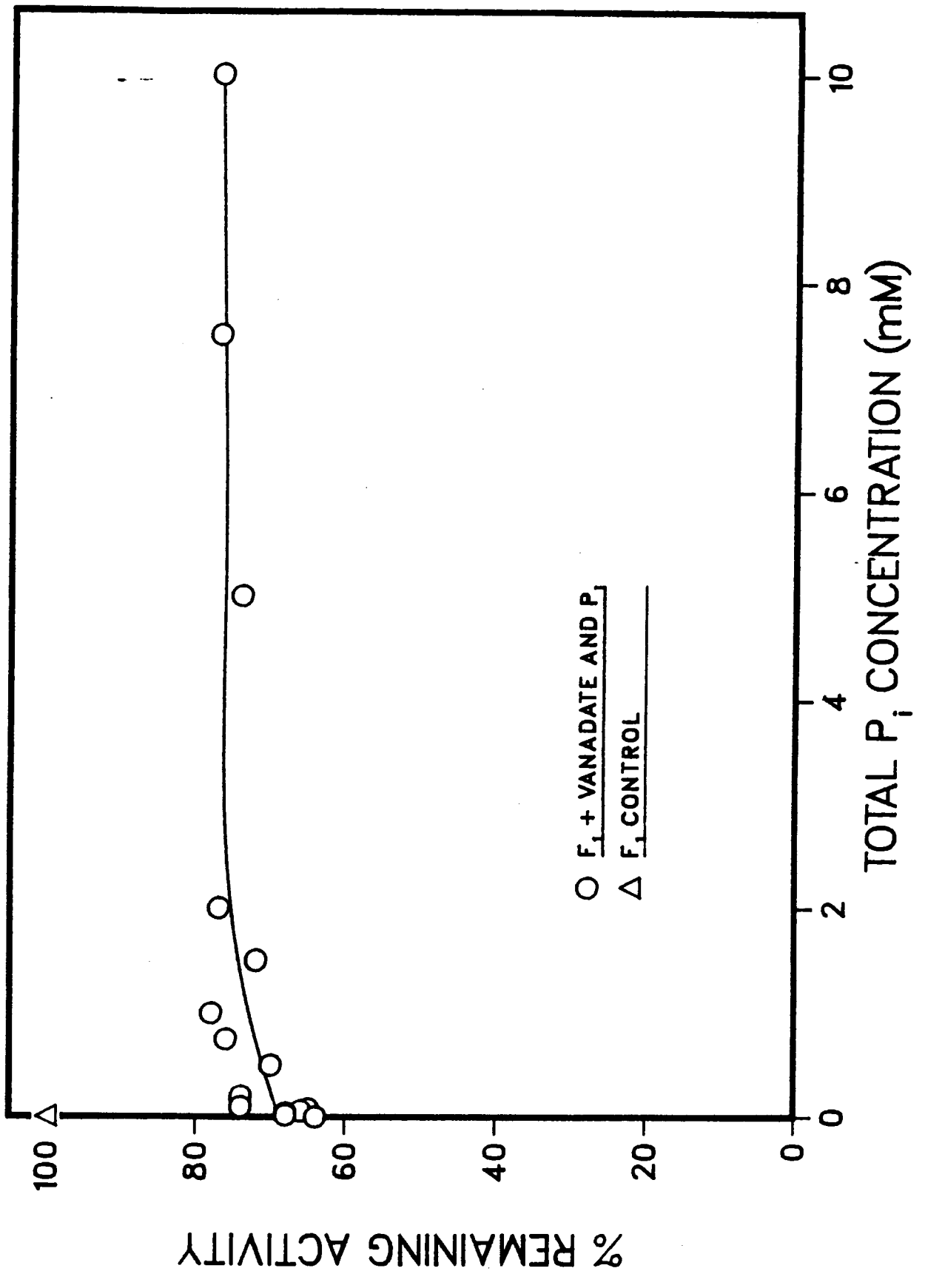
% REMAINING ACTIVITY
100
80
60
40
20
0
0
2
4
6
8
10
TOTAL P_i CONCENTRATION (mM)
○ F_1 + VANADATE AND P_i
△ F_1 CONTROL

Figure 11. **Inhibition of $^{32}P[P_i]$ binding to F_1 by vanadate.**

F_1 was incubated with 50 (○) or 75 μM (Δ) phosphate and various amounts of vanadate in solution containing 2 mM $MgSO_4$ and 50 mM Tris-OAc at pH 7.5. Fitting of equation A (shown in Appendix 1) to the data in the figure resulted in K_p, K_v and K_{vp} the values of 34.9 μM, 15.2 μM and 126.0 μM respectively. Calculated data using these constants are represented by solid lines in the figure. [Vi] was calculated using $K_2 = 0.21\ mM^{-1}$ and $K_4 = 0.37\ mM^{-3}$.

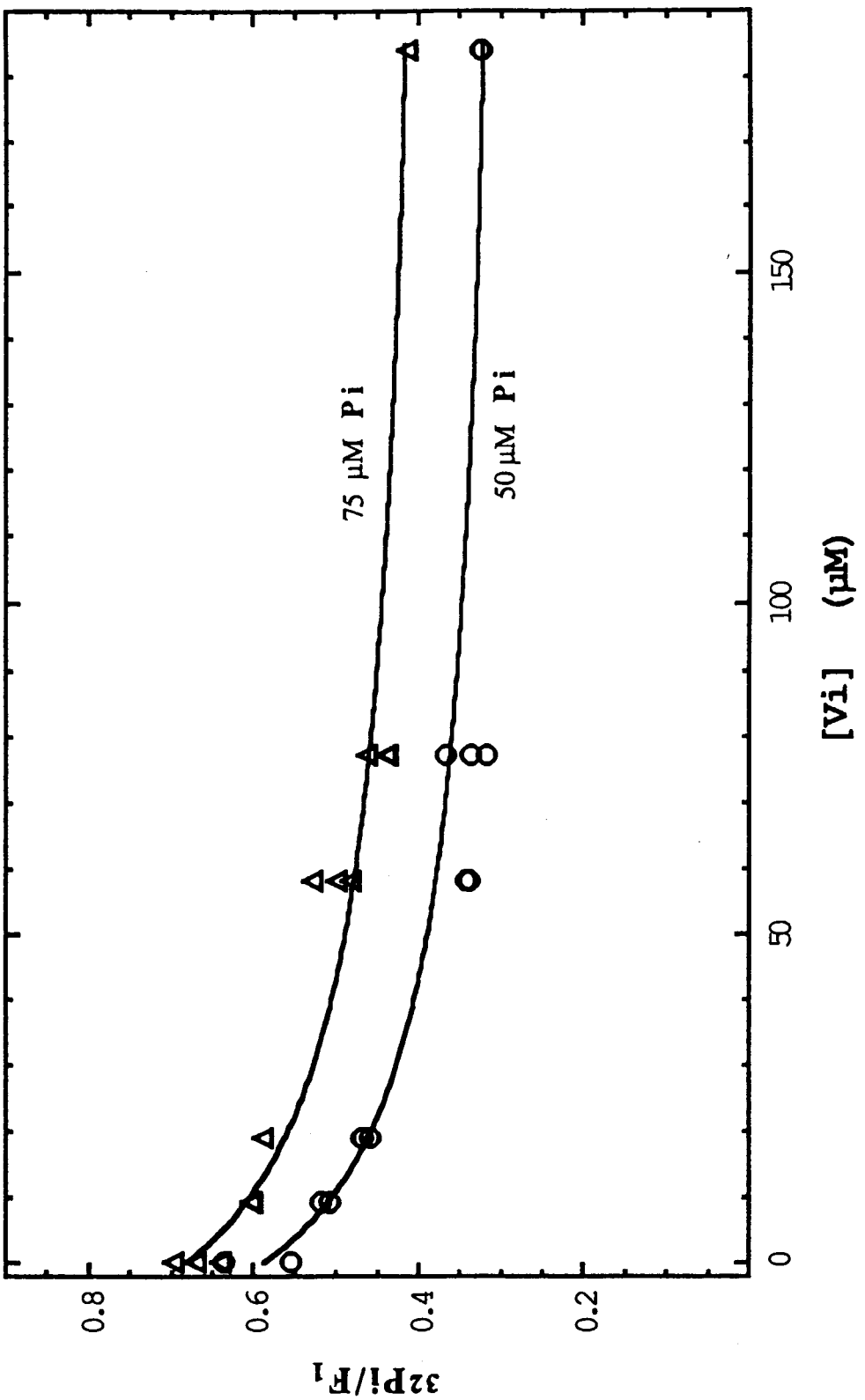
0.8
0.6
0.4
0.2
0
50
100
150
[Vi] (μM)
32Pi/F1
75 μM Pi
50 μM Pi

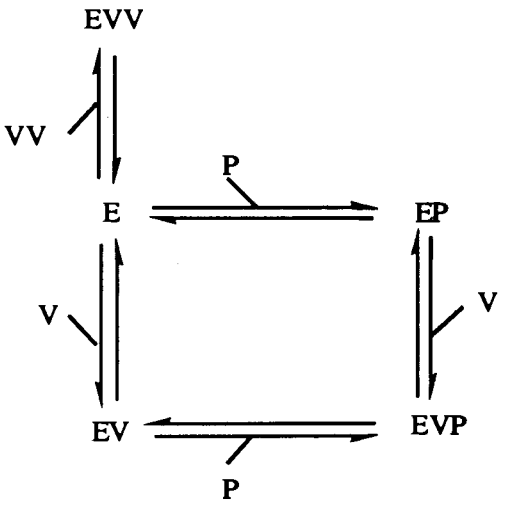

$K_p = 34.9 \pm 1.8$ μM

$K_{vp} = 126 \pm 11$ μM

$K_v = 15.2 \pm 3.4$ μM

E : F_1

P : Pi

V : Vi

Figure 12

Model for simultaneous binding of P_i and Vi to F_1

(C) Kinetics of inhibition of F_1 by vanadate

Vanadate inhibits F_1 catalyzed ATP hydrolysis, but in the submicromolar range, the inhibition is insignificant. At the millimolar vanadium concentrations used in this study, vanadium chemistry is complicated by the existence of monovanadate and polymeric forms of vanadate at neutral pH. At pH 7.5, which was the pH used in the assay system, three major forms of vanadate were in equilibrium: mono-, di-, and tetravanadate. The equilibrium constants for these three species were determined from NMR spectroscopic measurements. Since vanadate oxyanions complex easily with molecules bearing hydroxyl or carboxyl groups (48, 49, 50, 51), the formation constants for the vanadate species were determined in buffer solutions with or without substances present in the assay mixture. The candidates for complexing vanadate in the solution were PEP, Tris and acetate ions. The effect of the presence of ATP was also investigated since AMP and ADP are known to chelate monovanadate (52). The formation constants determined from NMR spectra are summarized in Table IIA and IIB.

The presence of coupling enzymes (PK and LDH) as well as substances such as NADH and PEP, did not affect the equilibrium constants (cf. lanes # 2,3 and 4,5,6 in Table IIB). Addition of MgATP to the solution seemed not to change the equilibrium by a significant extent under the conditions of the measurement. However, both K_2 and K_4 were slightly higher with MgATP added. The increment was not solely due to change of the ionic strength since no such dependence was observed when MgATP concentration was raised from 0.5 to 5 mM. Similarly, when 5 or 10 mM P_i

Table IIA

NMR determination of formation constants for V_2 and V_4 in solution containing 4.3 mM $MgCl_2$

	[V] (mM)	LIGANDS IN SOLUTION*	K_2 (mM^{-1})	K_4 (mM^{-3})	AVERAGE K_2 (mM^{-1})	AVERAGE K_4 (mM^{-3})
1	0.5	--	0.25	0.84	0.28 ± 0.02	0.80 ± 0.04
2	1.5	--	0.31	0.77		
3	2.5	--	0.29	0.79		
3	2.5	--	0.29	0.79	0.32 ±0.02	0.86 ± 0.07
4	2.5	0.5mM MgATP	0.32	0.82		
5	2.5	1.0mM MgATP	0.35	0.98		
6	2.5	2.5mM MgATP	0.31	0.84		
7	2.5	5.0mM MgATP	0.32	0.87		
8	0.5	5 mM P_i	0.30	0.75	0.30 ± 0.02	0.76 ± 0.11
9	1.5	5 mM P_i	0.28	0.66		
10	2.5	5 mM P_i	0.33	0.88		
11	0.5	10 mM P_i	0.30	0.85	0.29 ± 0.02	0.80 ± 0.09
12	1.5	10 mM P_i	0.26	0.70		
13	2.5	10 mM P_i	0.30	0.86		
14	2.5	1 mM MgATP + 5 mM P_i	0.30	0.78	0.30	0.78
15	2.5	1 mM MgATP + 10 mM P_i	0.27	0.73	0.27	0.73

[V] = total vanadium atom concentration

* Solution was the assay mixture at pH 7.5 containing 50 mM Tris-OAc, 4.3 mM $MgCl_2$, 3.33 mM K^+-PEP, 0.21 mM NADH, 100 µg PK, 60 µg LDH, and 20 µg SOD.

Table IIB

NMR determination of formation constants for V_2 and V_4 in solution containing 2 mM $MgCl_2$

	[V] (mM)	LIGANDS IN SOLUTION*	K_2 (mM^{-1})	K_4 (mM^{-3})	AVERAGE K_2 (mM^{-1})	AVERAGE K_4 (mM^{-3})
1	1.0	$MgCl_2$ ONLY†	0.28	0.40		
2	1.5	$MgCl_2$ ONLY†	0.20	0.25		
3	2.5	$MgCl_2$ ONLY†	0.23	0.34		
4	1.0	ASSAY MIXTURE	0.21	0.35		
5	1.5	ASSAY MIXTURE	0.23	0.41	0.21 ± 0.02	0.37 ± 0.03
6	2.5	ASSAY MIXTURE	0.20	0.35		
7	2.5	ASSAY MIXTURE + 5 mM MgATP	0.29	0.52		
8	2.5	ASSAY MIXTURE + 0.5 mM MgATP	0.24	0.46		

[V] = total vanadium atom concentration

* Solution contained 50 mM Tris-OAc at pH 7.5.

† 2 mM $MgCl_2$ added to the solution.

Assay mixture : contained the same ingredients as in the solution described in Table IIA but with only 2 mM $MgCl_2$.

was present in the solution, with or without MgATP, the equilibrium constants did not vary significantly.

The concentration distribution curves of Vi, V_2 and V_4 with respect to total vanadium atom concentration are plotted in Figure 13A using values of K_2 and K_4 of 0.28 mM^{-1} and 0.80 mM^{-3} respectively, and in Figure 13B using values of K_2, K_4 of 0.21 mM^{-1} and 0.37 mM^{-3} respectively. It can be seen from the graphs that monovanadate predominates within the spectrum of vanadium concentrations investigated; on the other hand, the amounts of divanadate and tetravanadate become significant only when total vanadium is in the millimolar range.

In addition to the the speciation of vanadate, the kinetic study is further complicated by the catalytic property of the enzyme; the double reciprocal plot of the enzyme activity is nonlinear (Figure 14) due to the catalytic cooperativity of the enzyme. The enzyme assay therefore had to be made over a suitable substrate concentration range to provide a linear slope for the use in the secondary plot and data analysis. Another complication in this study is that vanadate oxidizes NADH in the assay mixture via a mechanism that involves superoxide radical formation (53). SOD was therefore added to the assay mixture to interrupt such process. Presence of SOD did not affect the F_1 catalyzed reaction.

The kinetic results of vanadate inhibition of F_1 are presented in the double reciprocal plot in Figure 15 with the substrate concentration range between 0.1 mM and 0.0193 mM. At this low and narrow concentration range, the enzyme catalysis follows Michaelis-Menton kinetics (20, 54) and gives linear graphs in the double reciprocal plots as shown in the figure.

Figure 13A. **Distribution curve for Vi, V_2 and V_4 as a function of total vanadium atom concentration in solution with 4.3 mM $MgCl_2$.**

(Formation constants from Table IIA: K_2 = 0.28 mM^{-1} and K_4 = 0.80 mM^{-3})

Figure 13B. **Distribution curve for Vi, V_2 and V_4 as a function of total vanadium concentration in solution with 2 mM $MgCl_2$.**

(Formation constants from Table IIB: K_2 = 0.21 mM^{-1} and K_4 = 0.37 mM^{-3})

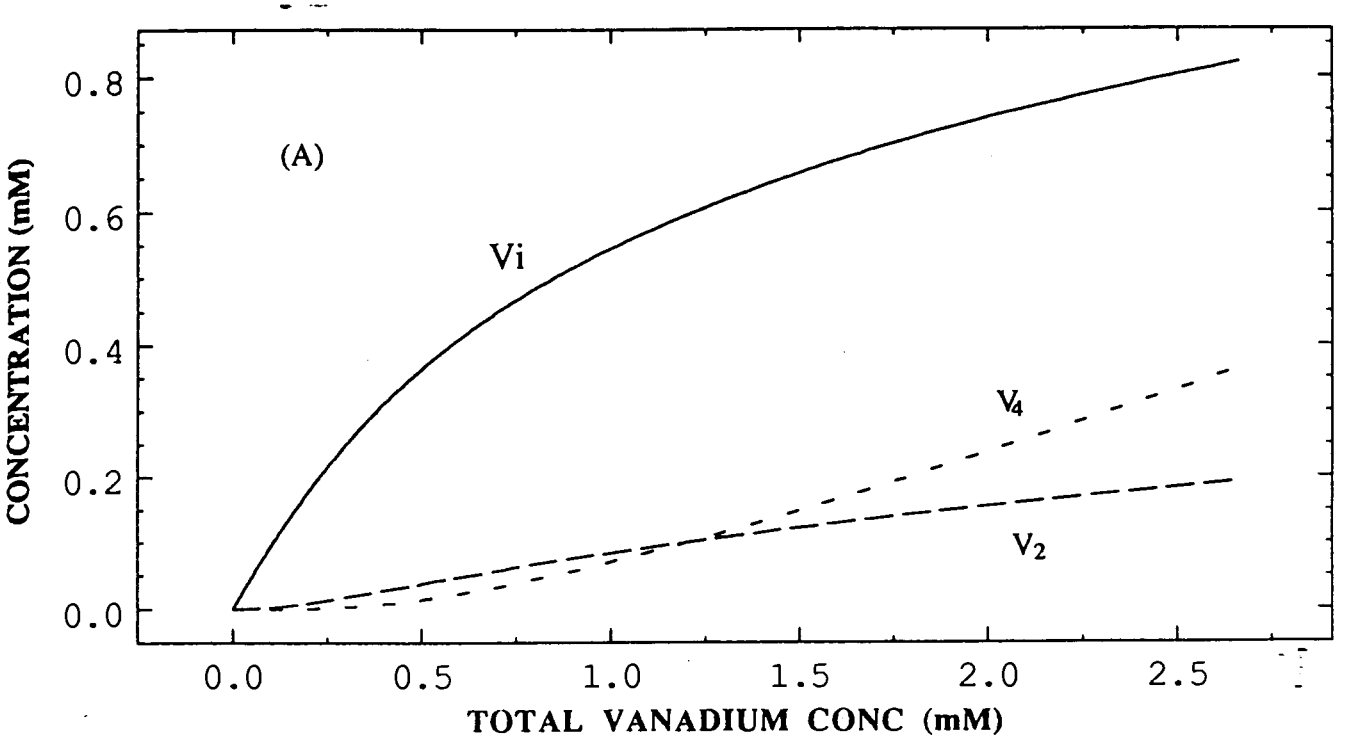
(A)
Vi
V4
V2
CONCENTRATION (mM)
0.0
0.2
0.4
0.6
0.8
0.0
0.5
1.0
1.5
2.0
2.5
TOTAL VANADIUM CONC (mM)

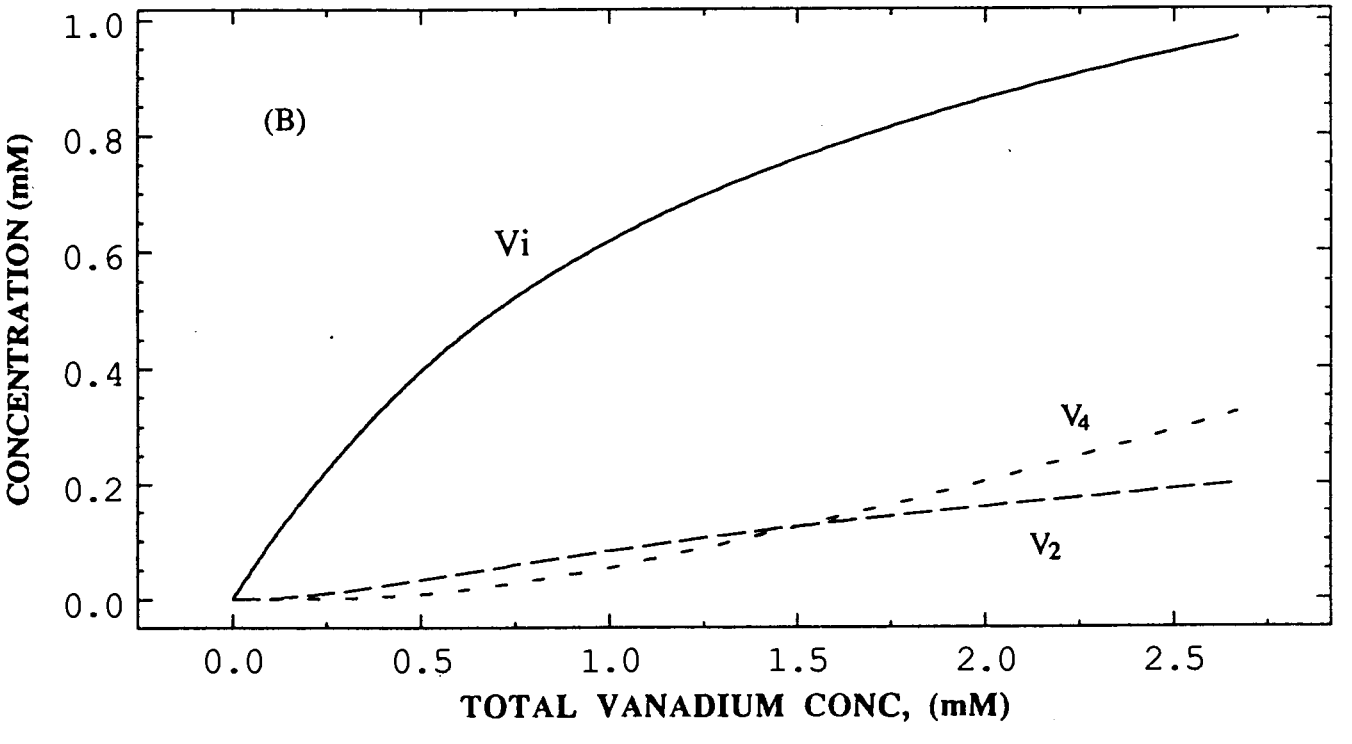
(B)
Vi
V4
V2
CONCENTRATION (mM)
0.0
0.2
0.4
0.6
0.8
1.0
0.0
0.5
1.0
1.5
2.0
2.5
TOTAL VANADIUM CONC, (mM)

Figure 14. **The dependence of the rate of F_1-catalyzed ATP hydrolysis on MgATP concentration.**

Activity of F_1 [3,0] at a concentration of 0.5 mg/ml was assayed at various MgATP concentration. Enzyme aliquots of 4 μL were added to assay mixtures containing 50 mM Tris-OAc, 2 mM $MgCL_2$, 3.3 mM K^+-PEP, 0.21 mM NADH, 100 μg PK, 60 μg LDH, and the indicated amounts of MgATP at pH 7.5 to initiate the reaction. Rate of ATP hydrolysis was determined after steady state was reached. (A) rate vs. [MgATP], (B) double reciprocal plot of the data shown in (A).

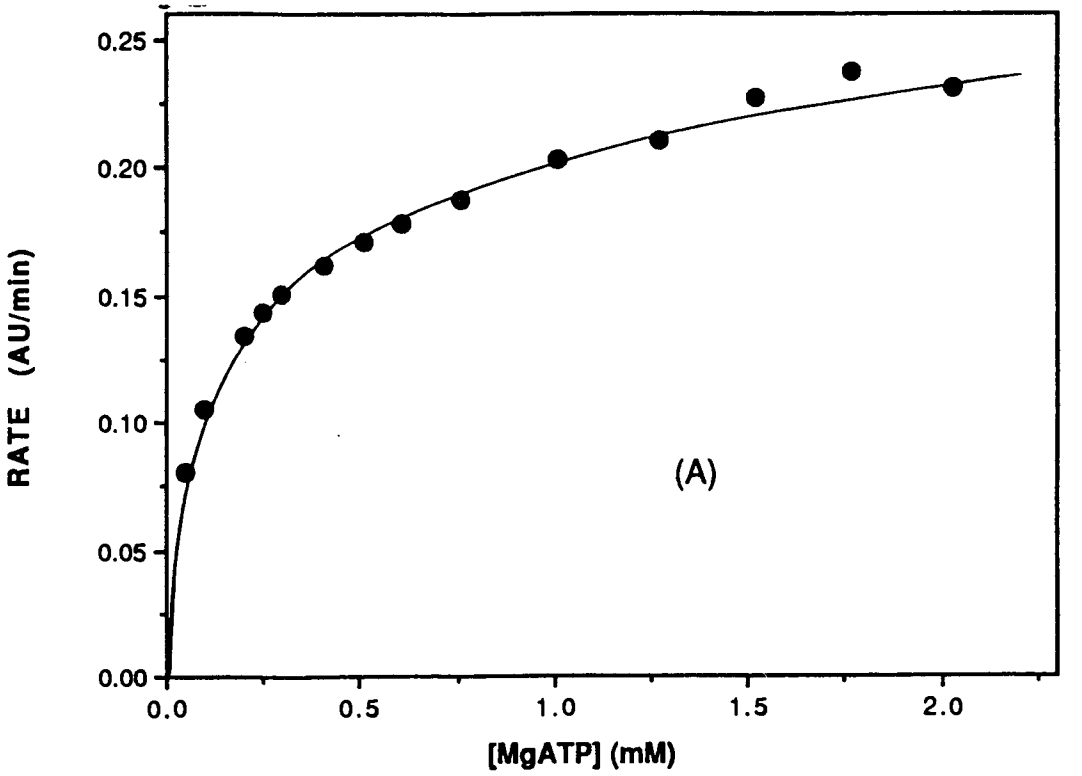
RATE (AU/min)
0.25
0.20
0.15
0.10
0.05
0.00
0.0
0.5
1.0
1.5
2.0
[MgATP] (mM)
(A)

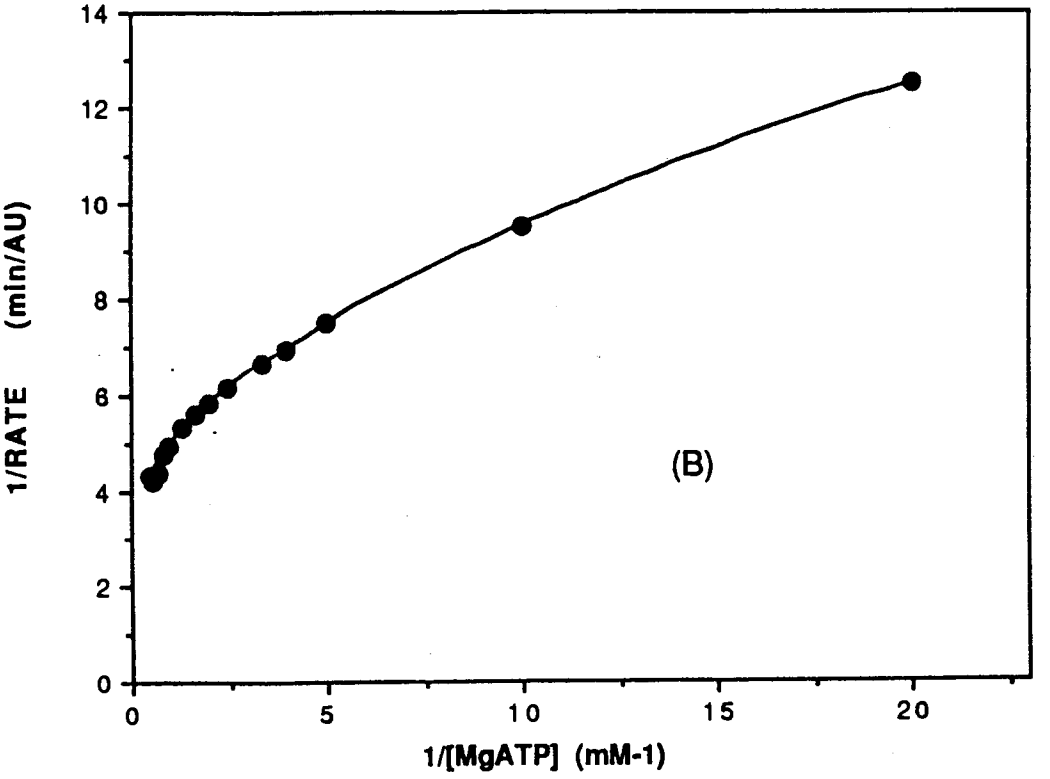
1/RATE (min/AU)
14
12
10
8
6
4
2
0
0
5
10
15
20
1/[MgATP] (mM-1)
(B)

Figure 15. **Double reciprocal plots of the dependence of the rate of F_1-catalyzed ATP hydrolysis on MgATP concentration at various fixed concentrations of vanadate.**

F_1 was prepared as [3,0] at a concentration of 0.57 mg/mL. Enzyme aliquots of 5 μL were added to initiate ATP hydrolysis in assay mixtures containing 50 mM Tris-OAc, 2 mM $MgCl_2$, 4 mM K^+-PEP, 100 μg PK, 60 μg LDH, 20 μg SOD, 0.21 mM NADH, and indicated amounts of MgATP and vanadate at pH 7.5. The rate shown in the figure was the highest linear rate obtained from the assay.

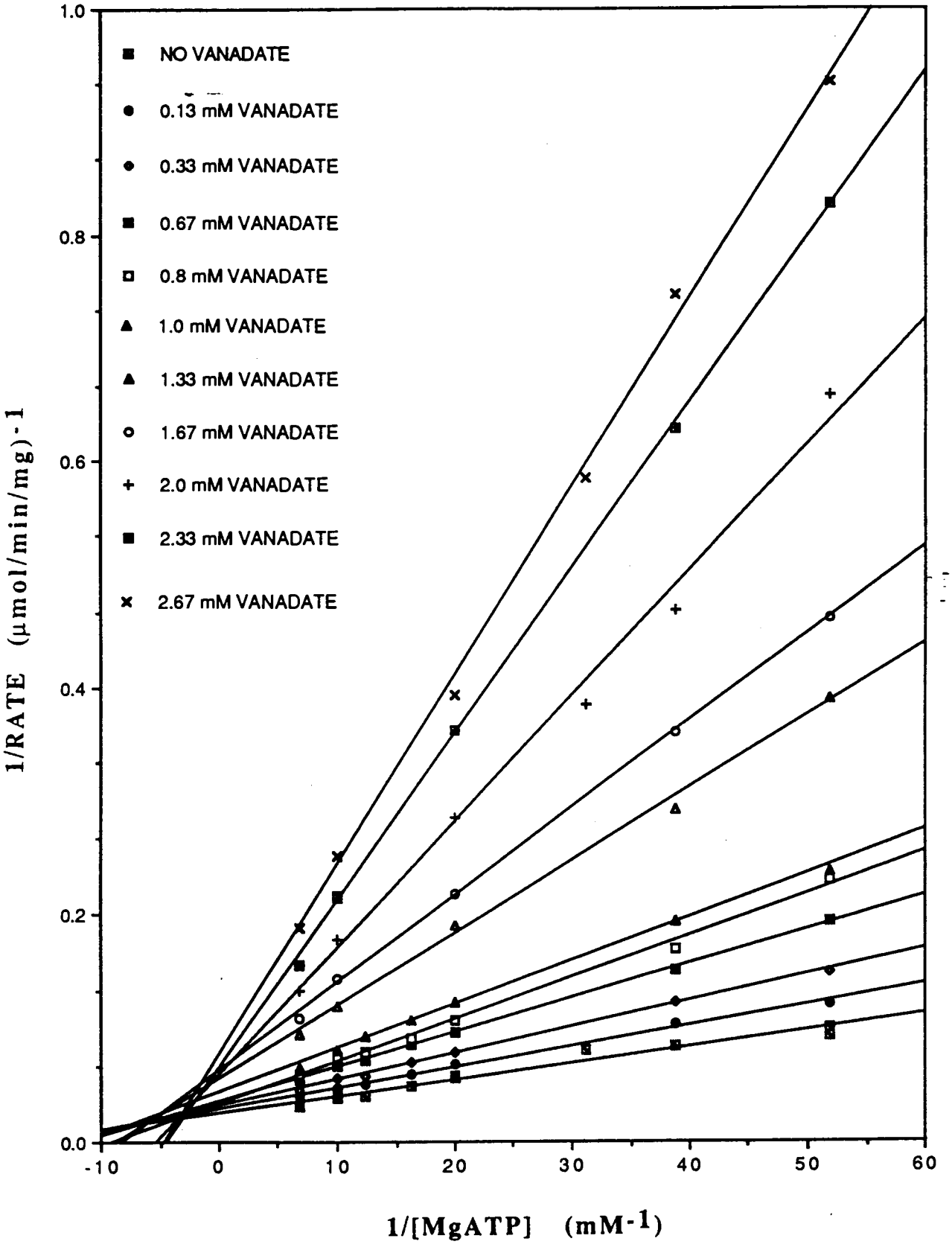
NO VANADATE
0.13 mM VANADATE
0.33 mM VANADATE
0.67 mM VANADATE
0.8 mM VANADATE
1.0 mM VANADATE
1.33 mM VANADATE
1.67 mM VANADATE
2.0 mM VANADATE
2.33 mM VANADATE
2.67 mM VANADATE
1.0
0.8
0.6
0.4
0.2
0.0
-10
0
10
20
30
40
50
60
1/RATE (µmol/min/mg)-1
1/[MgATP] (mM-1)

The regression lines drawn through the experimental data corresponding to lower vanadate concentrations (0-0.8 mM) intersect at a point above the reciprocal of 0.2 mM MgATP. However, the regression lines for higher inhibitor concentration do not converge to this intersection point. The slopes determined from Figure 15 were graphed in the secondary plot shown in Figure 16. The horizontal axis indicates concentrations of total vanadium, monovanadate, divanadate, or tetravanadate that were calculated with the formation constants in Table IIB (K_2 = 0.21 mM^{-1} and K_4 = 0.37 mM^{-3}). The statistical analysis of the slope determination using linear regression was performed as described by Wilkinson (55). Selected duplicate assays were performed and the largest deviation observed was 7%. It is expected that if a particular species is the inhibitor, a straight line should be obtained in the secondary plot. This is not observed in Figure 16. Graphs 16B and C show linearity at low monovanadate and divanadate concentrations, but the rise in the slope is more rapid at higher concentrations. On the other hand, the increase in the slope in Figure 16D appears to be linearly proportional to the tetravanadate concentration except at the low concentration range.

Direct kinetic analysis, as shown above, cannot pinpoint the species of vanadate responsible for inhibiting F_1. However, it is possible to test by other means whether divanadate is one of the inhibitors. This was achieved by introducing P_i into the assay mixture containing vanadate. P_i condenses readily with Vi, to form the phosphoryl-vanadate (P-V) anhydride which is a divanadate analog; formation constant of the molecule is 5.8 M^{-1} at pH 7.98 (56). The formation of P-V will increase the total concentration of divanadate and its analog phosphovanadate (V_2 and

Figure 16. **Secondary slope plot for Figure 15.**

The error bar shown in (A)-(D) were obtained from statistical analysis of the determination of the slopes in Figure 15.

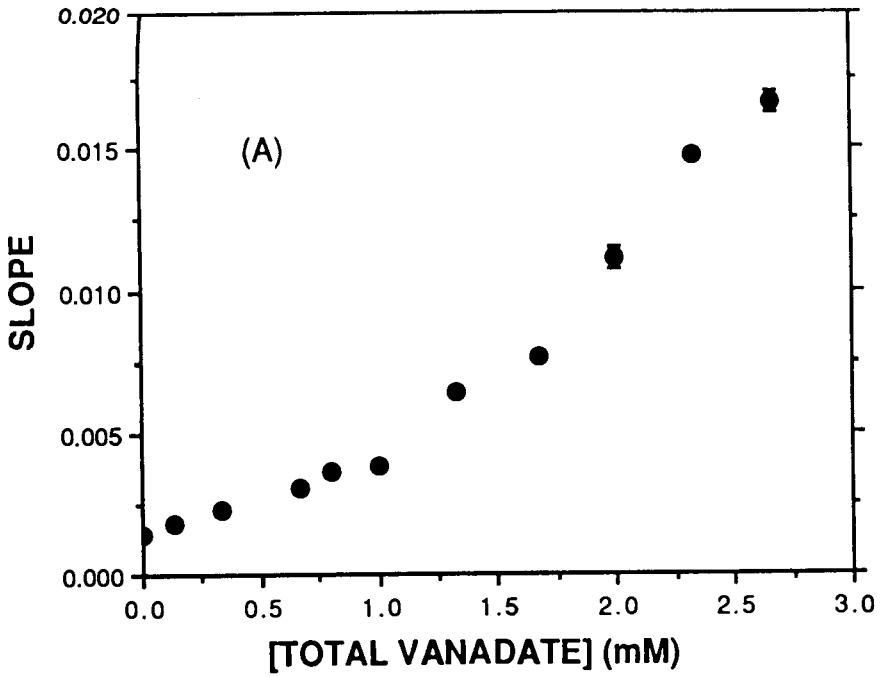
(A)
SLOPE
0.020
0.015
0.010
0.005
0.000
0.0
0.5
1.0
1.5
2.0
2.5
3.0
[TOTAL VANADATE] (mM)

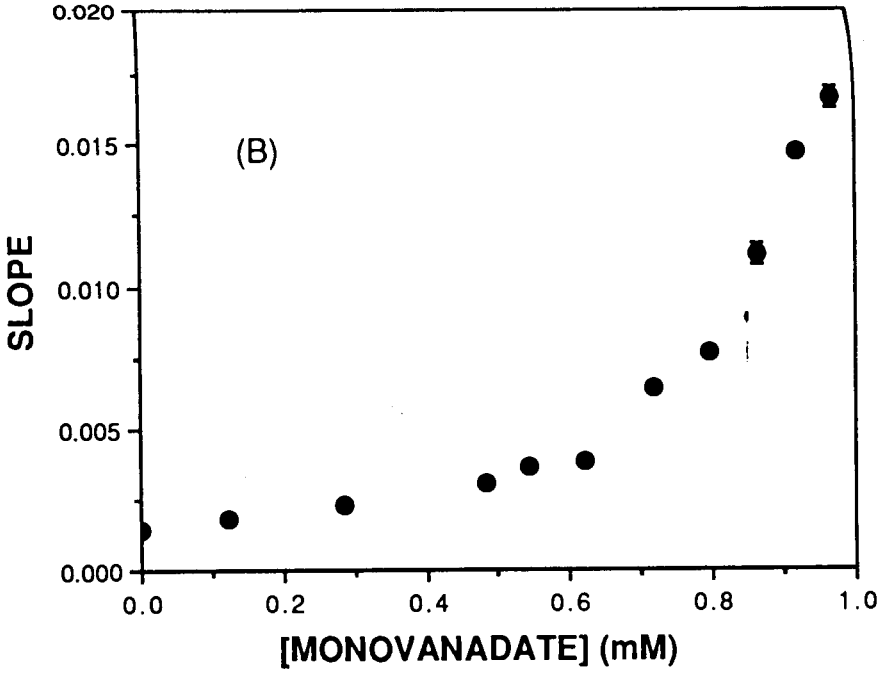
(B)
SLOPE
0.020
0.015
0.010
0.005
0.000
0.0
0.2
0.4
0.6
0.8
1.0
[MONOVANADATE] (mM)

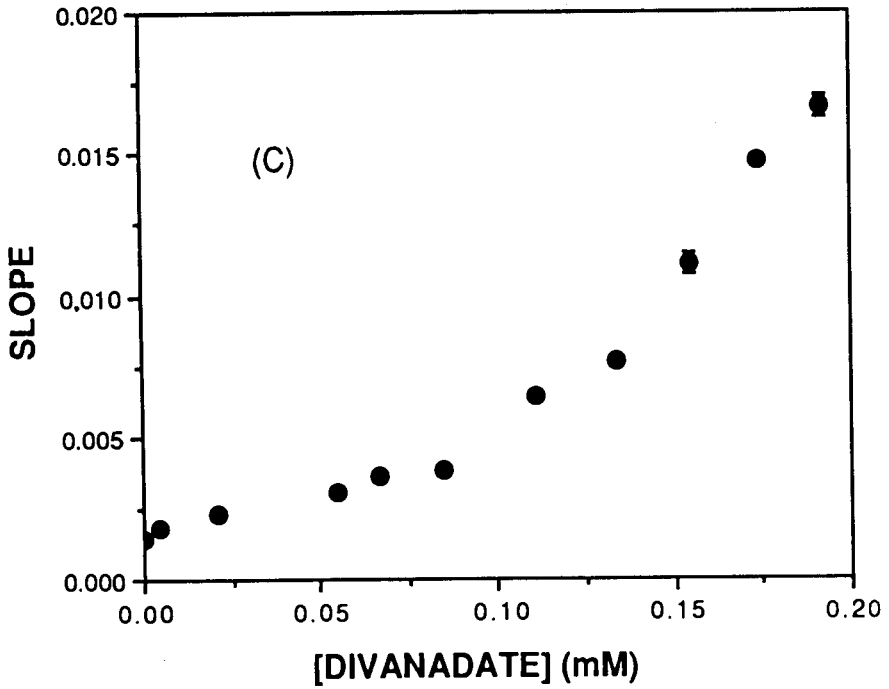
(C)
SLOPE
0.020
0.015
0.010
0.005
0.000
0.00
0.05
0.10
0.15
0.20
[DIVANADATE] (mM)

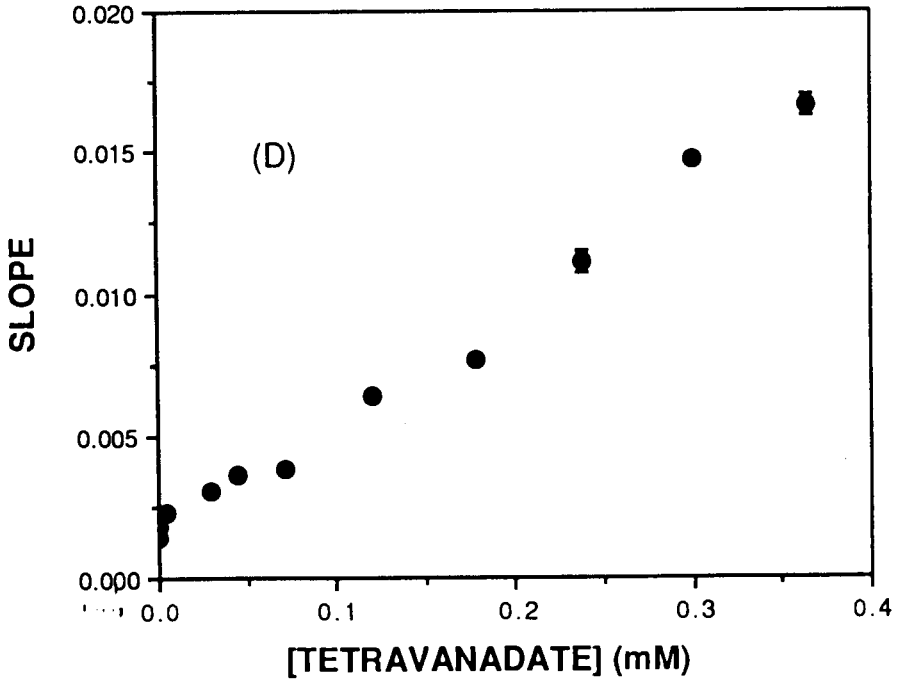
(D)
SLOPE
0.020
0.015
0.010
0.005
0.000
0.0
0.1
0.2
0.3
0.4
[TETRAVANADATE] (mM)

P-V) in the solution. As shown earlier in Table IIA, addition of 5 mM or 10 mM P_i did not alter the K_2 and K_4 values. Thus the effect of introducing P_i to vanadate-inhibited F_1-catalyzed ATP hydrolysis will reflect the result of increasing concentration of phosphovanadate while maintaining a constant concentration of divanadate. An observed increase in inhibition, which could be attributed to phosphovanadate, would support the hypothesis that divanadate is the inhibitor.

P_i by itself can either enhance or decrease F_1 activity depending on the concentration present (47). An appropriate P_i concentration to be added to the assay mixture should therefore be decided beforehand. It was found that under the experimental conditions used, 5-10 mM was the concentration of P_i that enhanced the enzyme activity to the greatest extent (determined at 2 mM MgATP, shown in Table III). However, this observed enhancement of rate of ATP hydrolysis was dependent on the substrate concentration in the assay mixture. Table III shows that although 5 mM and 10 mM P_i increased the enzyme activity at 2 mM MgATP, the enhancement was not observed at 0.2 mM MgATP. Similarly, results in Figure 17 indicate that with 10 mM P_i in the mixture (□), and at ATP concentrations below 0.8 mM, the rate of ATP hydrolysis was actually lower than when P_i was omitted (▲). At higher substrate concentration, the presence of P_i increased the rate of hydrolysis. Figure 17 also shows the effect of P_i on inhibition of F_1 by vanadate. P_i and vanadate together (●) inhibited the enzyme more than vanadate alone (X). The enhancement of inhibition was again ATP concentration dependent; the effect diminished above 2.5 mM substrate concentration.

Figure 17. **Double reciprocal plot of the dependence of the rate of F_1-catalyzed ATP hydrolysis on MgATP concentration in the presence of phosphate, vanadate, or phosphate plus vanadate.**

Activity was determined using 0.6 mg/mL F_1 prepared as F_1[3,0]. The assay mixture was the same as that described in Figure 15 but with varying amounts of ATP as shown in the figure. Four assays were performed simultaneously with 5 μL F_1 added to assay mixtures containing either no added vanadate or P_i (▲), 10 mM P_i (□), 0.2 mM vanadate (X), or 10 mM P_i and 0.2 mM vanadate (●).

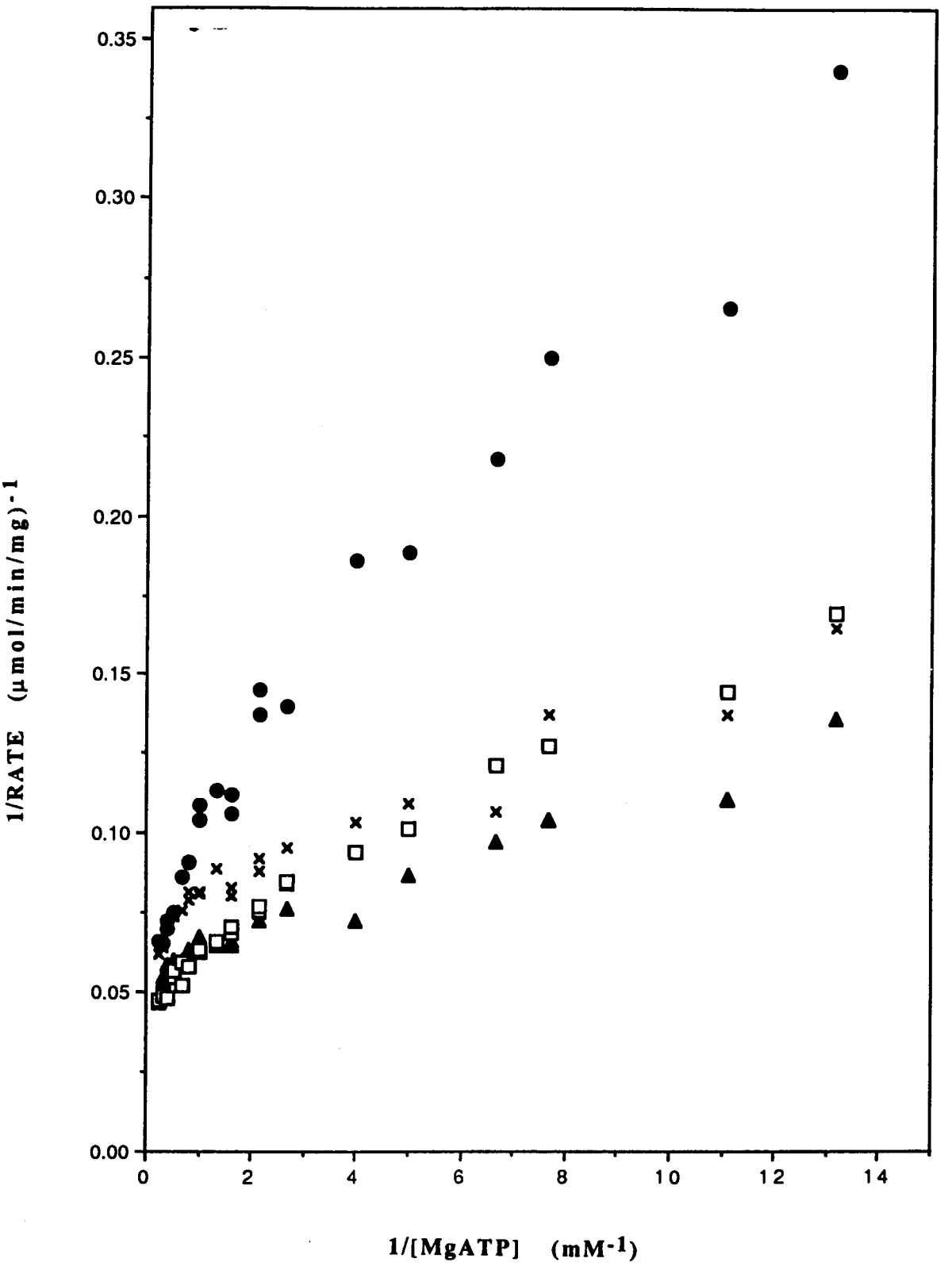
0.35
0.30
0.25
0.20
0.15
0.10
0.05
0.00
0
2
4
6
8
10
12
14
1/RATE (µmol/min/mg)-1
1/[MgATP] (mM-1)

Table III

Effect of P_i on F_1-catalyzed ATP hydrolysis*

[P_i] (mM)	Rate of ATP hydrolysis (AU/min)	
	2 mM MgATP	0.2 mM MgATP
0	0.1669	0.1056
2.5	0.1688	0.09375
5	0.1743	0.08871
10	0.1698	0.08753
15	0.1647	0.08664
20	0.1648	0.08915
25	--	0.08478

* Assay conditions were as described with Figure 15

When a similar experiment was performed with PP_i or AMP, no such enhancement of vanadate inhibition was observed.

In Figures 19 and 20, inhibition of F_1 by various concentrations of vanadate over 0.3-2 mM ATP concentration range was studied in the presence or absence of 10 mM P_i respectively. For easier comparison, the lines representing the lowest and the highest vanadate concentrations in Figure 19 were shown in Figure 18 (dotted lines) and vice versa in Figure 19. It can be seen from the graphs that P_i enhanced inhibition within the vanadate and ATP concentration range tested.

A similar experiment was performed but with ATP concentration fixed at 2 mM in the presence of 5 mM or 10 mM P_i and over a vanadate concentration range from 0.13 to 2.67 mM. Figures 20A and 20B summarize

Figure 18. **Inhibition of F_1-catalyzed ATP hydrolysis by vanadate.**

ATP hydrolysis was initiated with 5 µL of 0.86 mg/mL F_1 in an assay system containing 2 mM $MgCl_2$, 3.3 mM K^+-PEP, 0.21 mM NADH, 100 µg Pk, 60 µg LDH, 20 µg SOD and indicated amounts of MgATP. The solution was buffered at pH 7.5 with 50 mM Tris-OAc and contained also 0, 0.33, 0.47, 0.8, 1.13, 1.67 mM vanadate. Remaining activity was defined as :

$$\text{Remaining activity} = \frac{\text{rate of ATP hydrolysis in the presence of vanadate}}{\text{rate of ATP hydrolysis in the absence of vanadate}}$$

The broken lines in the figure are results taken from Figure 19. They are shown in this figure for easier comparison between the results in both graphs.

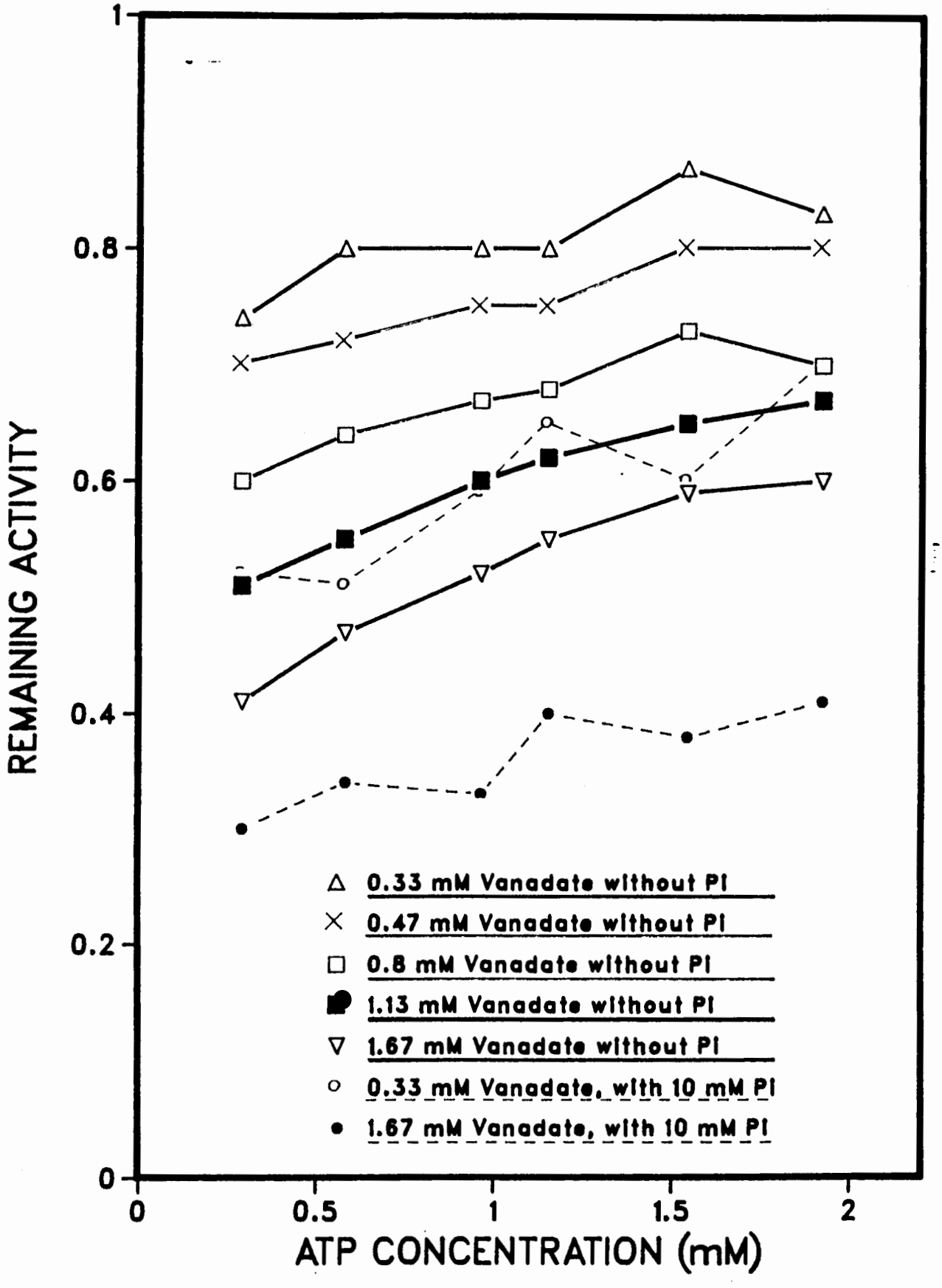
REMAINING ACTIVITY
1
0.8
0.6
0.4
0.2
0
0
0.5
1
1.5
2
ATP CONCENTRATION (mM)
0.33 mM Vanadate without PI
0.47 mM Vanadate without PI
0.8 mM Vanadate without PI
1.13 mM Vanadate without PI
1.67 mM Vanadate without PI
0.33 mM Vanadate, with 10 mM PI
1.67 mM Vanadate, with 10 mM PI

Figure 19. **Inhibition of F_1-catalyzed ATP hydrolysis by vanadate in presence of 10 mM P_i.**

The activity assay was the same as that described with Figure 18 except that the assay mixture contained 10 mM P_i. Remaining activity was calculated as:

$$\text{R.A.} = \frac{\text{rate of ATP hydrolysis in presence of vanadate and 10mM } P_i}{\text{rate of ATP hydrolysis in presence of 10mM Pi but no vanadate}}$$

The broken lines in this figure are the results taken from Figure 18. They are shown here for easier comparisons between these two figures.

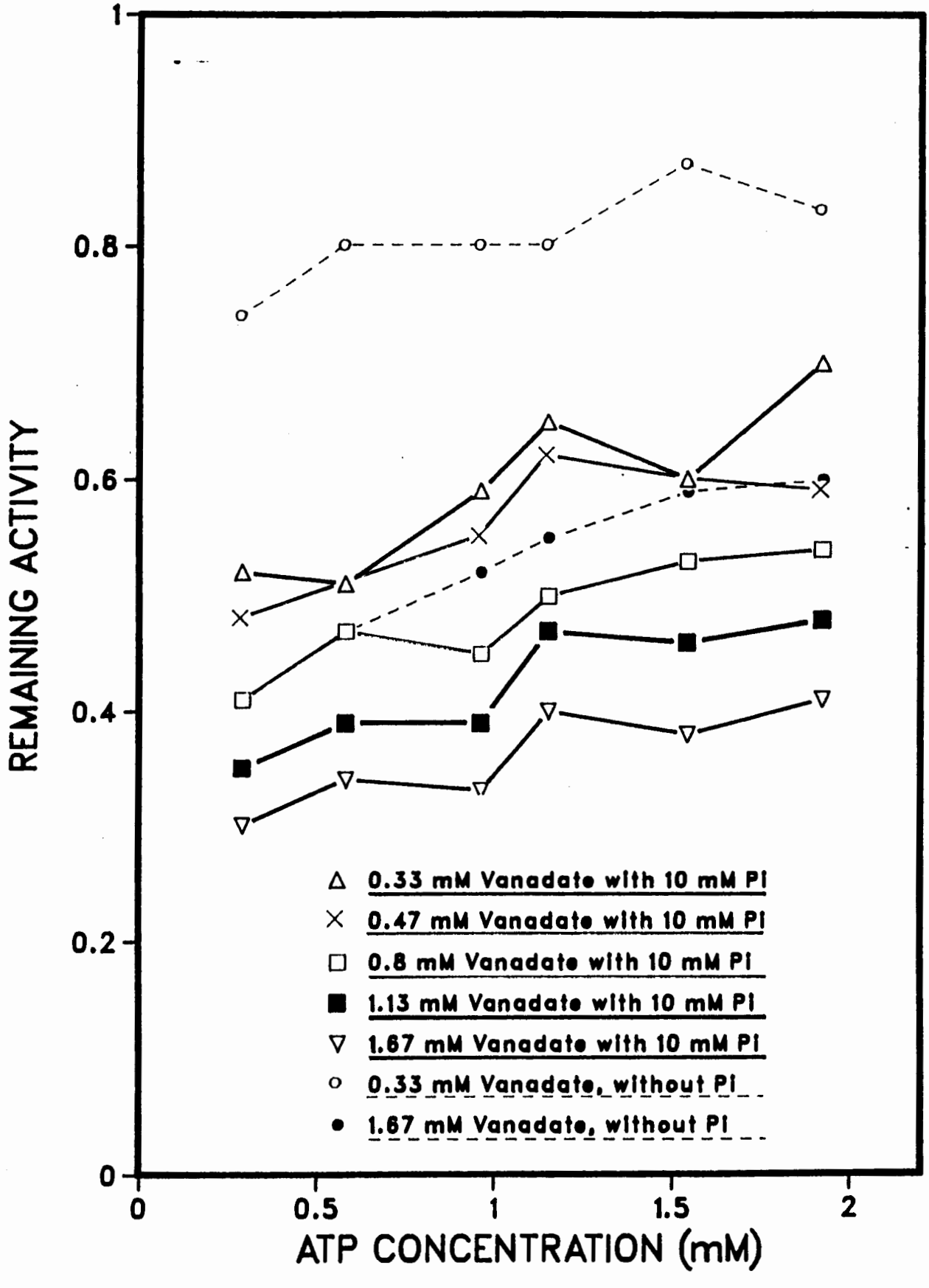
REMAINING ACTIVITY
1
0.8
0.6
0.4
0.2
0
0
0.5
1
1.5
2
ATP CONCENTRATION (mM)
0.33 mM Vanadate with 10 mM Pi
0.47 mM Vanadate with 10 mM Pi
0.8 mM Vanadate with 10 mM Pi
1.13 mM Vanadate with 10 mM Pi
1.67 mM Vanadate with 10 mM Pi
0.33 mM Vanadate, without Pi
1.67 mM Vanadate, without Pi

the results. The vertical axis in Figure 20A shows the amount of inhibition determined from the ratio of the hydrolysis rate in presence of both P_i and Vi to the hydrolysis rate of respective controls that had 5 or 10 mM P_i but no vanadate ($\frac{P_i+V}{P_i}$). Again, the results show that P_i enhanced vanadate-induced inhibition of F_1. The figure also demonstrates that the enhancement was proportional to the amount of P_i added; 10 mM P_i brought greater enhancement in inhibition than 5 mM P_i. When the ratio of the hydrolysis rate in the presence of P_i and Vi to the hydrolysis rate in the presence of vanadate alone was determined ($\frac{P_i+V}{V}$), an interesting result was obtained (Figure 20B). The y-axis in this case represents the extent of P_i induced enhancement in inhibition. At a fixed P_i concentration of 5 or 10 mM, the enhancement was not proportional to the amount of vanadate present, but reached a maximum value at 1 mM vanadate. The increase in inhibition was only proportional to the vanadate concentration below 1 mM, above this concentration the 'P_i effect' diminished.

Although vanadate binding to F_1 cannot be quantified easily, its rate of dissociation from the protein can be measured spectrophotometrically. This was done by following the recovery of enzyme activity after preincubating the enzyme with vanadate for some time, and diluting the incubation mixture into the assay solution. The final vanadate concentration in the assay mixture was too dilute to cause significant inhibition of F_1. The ATPase activity was slow initially but increased during the course of reaction until a steady state was reached. The first

Figure 20A. **Percentage inhibition of F_1-catalyzed ATP hydrolysis by vanadate as a function of vanadate concentration and in the presence of P_i -- "Vanadate Effect".**

ATP hydrolysis was initiated with 2 μL of 0.69 mg/mL F_1 in an assay system containing 2 mM $MgCl_2$, 3.3 mM K^+-PEP, 0.21 mM NADH, 100 μg PK, 60 μg LDH, 15 μg SOD and 2 mM MgATP buffered at pH 7.5 with 50 mM Tris-OAc. The assay mixture also contained 0, 0.13, 0.33, 0.67, 0.8, 1.0, 1.33, 1.67, 2.0, 2.33, 2.67 mM vanadate and either with no P_i (△), 5 mM P_i (□), or 10 mM P_i (○). % Inhibition and remaining activity (R.A.) are defined as:

% Inhibition = 100% - % R.A.

$$\text{R.A.} = \frac{\text{reaction rate in presence of } P_i \text{ and vanadate}}{\text{reaction rate in presence of same amount of } P_i \text{ but no vanadate}}$$

Figure 20B. **Percentage inhibition of F_1-catalyzed ATP hydrolysis by vanadate as a function of vanadate concentration and in the presence of P_i -- "Phosphate Effect".**

The assay conditions were the same as those described with Figure 20A. % Inhibition and remaining activity are defined as:

% Inhibition = 100% - % R.A.

$$\text{R.A.} = \frac{\text{reaction rate in presence of vanadate and } P_i}{\text{reaction rate in presence of same amount of vanadate but no } P_i}$$

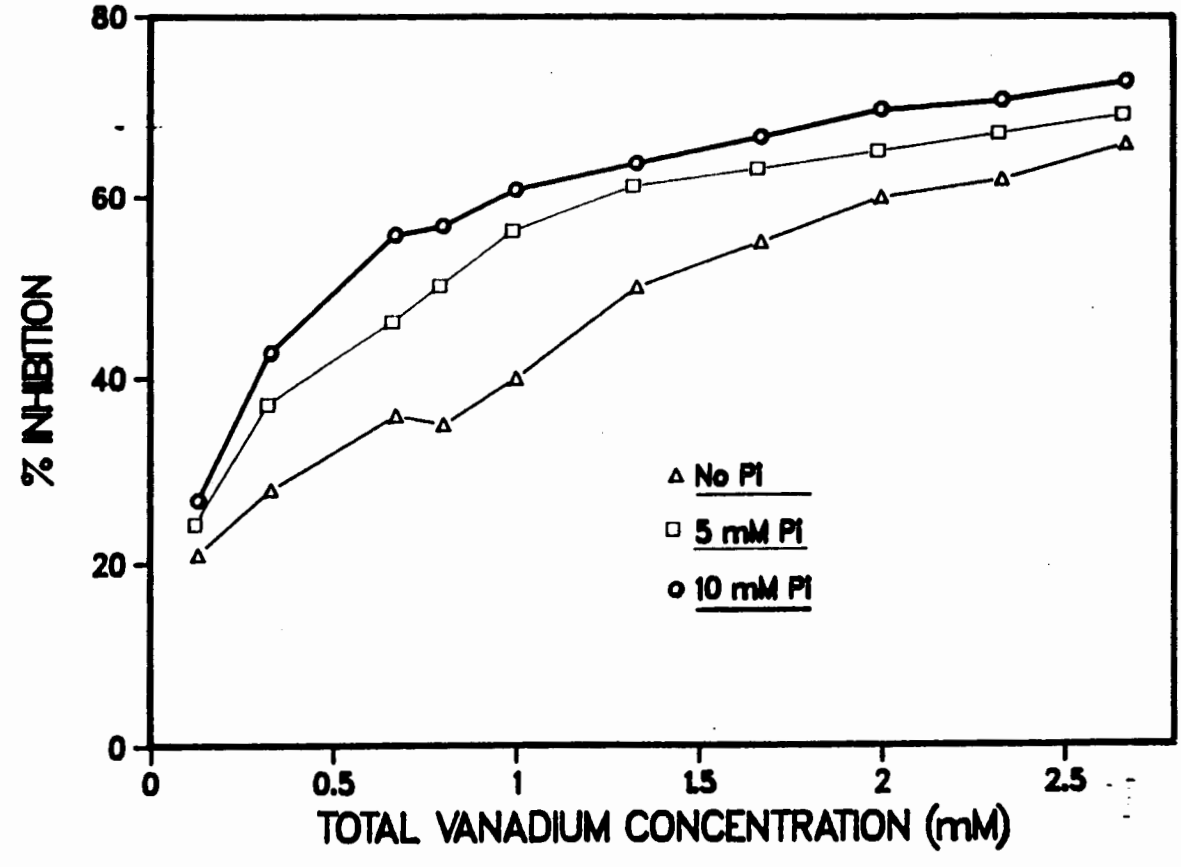
80
60
40
20
0
% INHIBITION
0
0.5
1
1.5
2
2.5
TOTAL VANADIUM CONCENTRATION (mM)
△ No Pi
□ 5 mM Pi
o 10 mM Pi

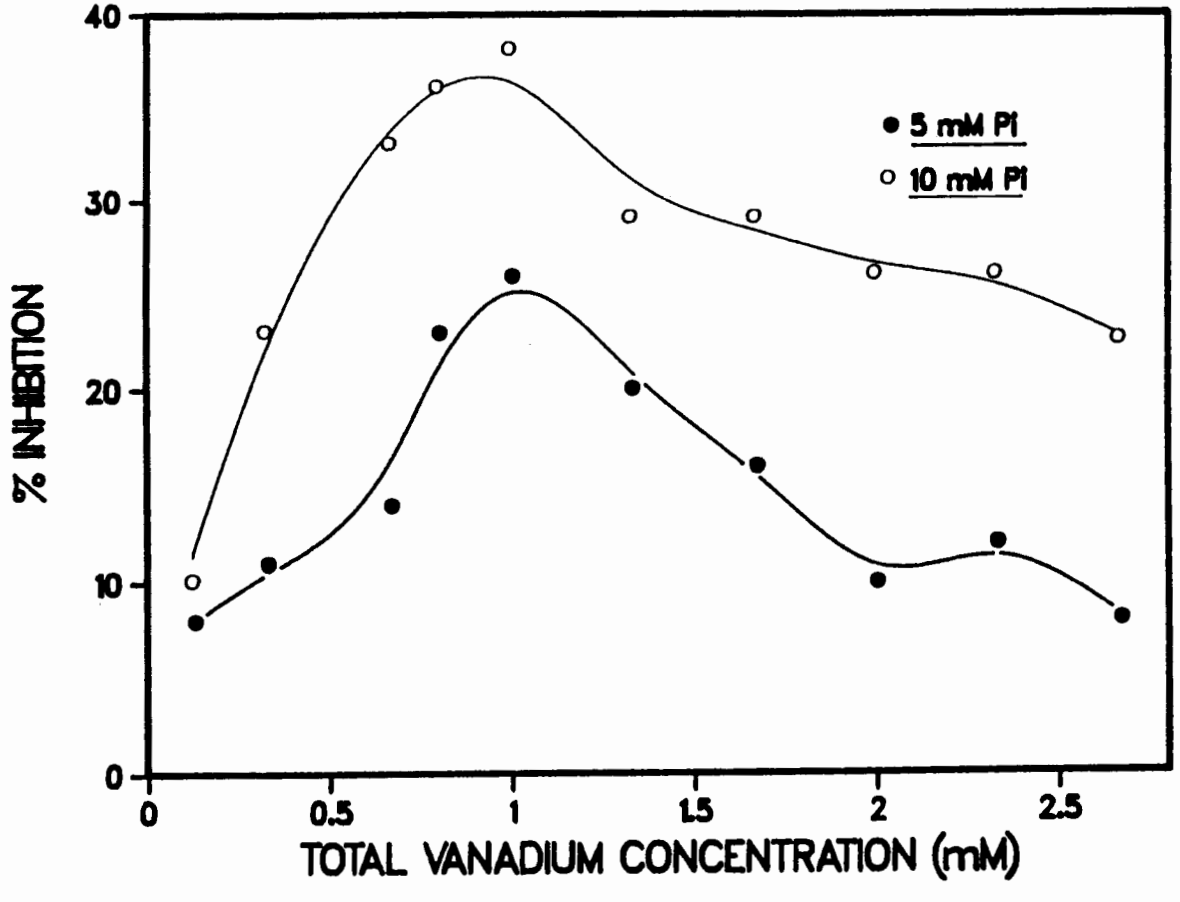
40
30
20
10
0
% INHIBITION
0
0.5
1
1.5
2
2.5
TOTAL VANADIUM CONCENTRATION (mM)
● 5 mM Pi
o 10 mM Pi

order rate constant for reactivation (which may correspond to that for dissociation of vanadate from F_1) could then be calculated by fitting the first order rate equation to the data. Derivation for the equation used for the fitting is shown in appendix 2. The observed rate constant for reactivation of the enzyme was found to be dependent on the concentration of the substrate ATP present (Figure 21A). A noteworthy result is that the rate constant for reactivation was unaffected by the presence of additional vanadate in the assay mixture, although the final, steady state enzyme activity was reduced. Figure 21B is the reciprocal plot of Figure 21A. The curving of the lines at low ATP concentration was due to the intrinsic lag in the enzyme activity observed even though no vanadate was associated with it. Such slow approach to steady state kinetics was more pronounced at low substrate concentration, and more severe with F_1[2,1] than F_1[3,0]. Although F_1 used in this experiment was prepared with three filled catalytic sites (F_1[3,0]), it is not unlikely that a small portion of the enzyme remained in the [2,1] conformation. Furthermore, slow conversion of F_1[3,0] to F_1[2,1] might have taken place as the lag became more apparent as incubation time increased. A separate experiment performed under similar conditions but completed in a shorter time (5 hr vs. 10 hr) showed no such curvature in the reciprocal plot (Figure 22B). The data in Figure 21 thus needed to be corrected for this discrepancy. Examining the activity of F_1 with no associated vanadate at low ATP concentration (0.028 mM) assayed at the end of the experiment, the apparent intrinsic k_{obs} of 0.0021 s^{-1} and 0.0016 s^{-1} were obtained for F_1 in the assay mixtures containing no vanadate and 0.5 mM vanadate

Figure 21. **Apparent rate constant for dissociation of vanadate from F_1 in assay mixtures containing no vanadate or 0.5 mM vanadate.**

F_1 was prepared as [3,0] at a concentration of approximately 0.7 mg/mL. The enzyme was incubated with 500 μM vanadate in the dark at ambient temperature for 2 hours before diluting 2 μL aliquots of the incubation mixture into 1498 μL assay solution containing 50 mM Tris-OAc, 2 mM $MgCl_2$, 3.3 mM K^+-PEP, 100 μg PK, 60 μg LDH, 20 μg SOD, 0.21 mM NADH and indicated amount of ATP at pH 7.5. For each ATP concentration, two assay mixtures were prepared; one without added vanadate (○) and the other with 0.5 mM vanadate (▲). The k_{obs} values were obtained as described in the text.

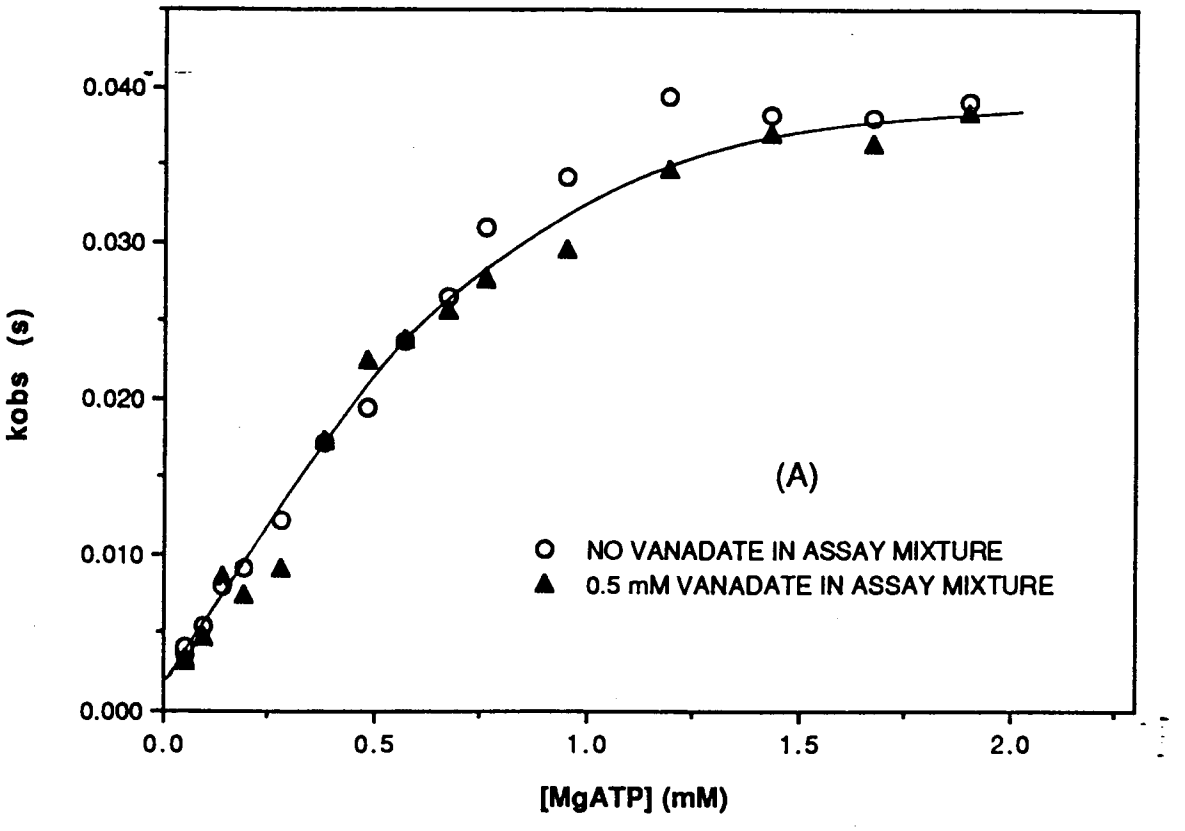
0.040
0.030
0.020
0.010
0.000
kobs (s)
0.0
0.5
1.0
1.5
2.0
[MgATP] (mM)
(A)
NO VANADATE IN ASSAY MIXTURE
0.5 mM VANADATE IN ASSAY MIXTURE

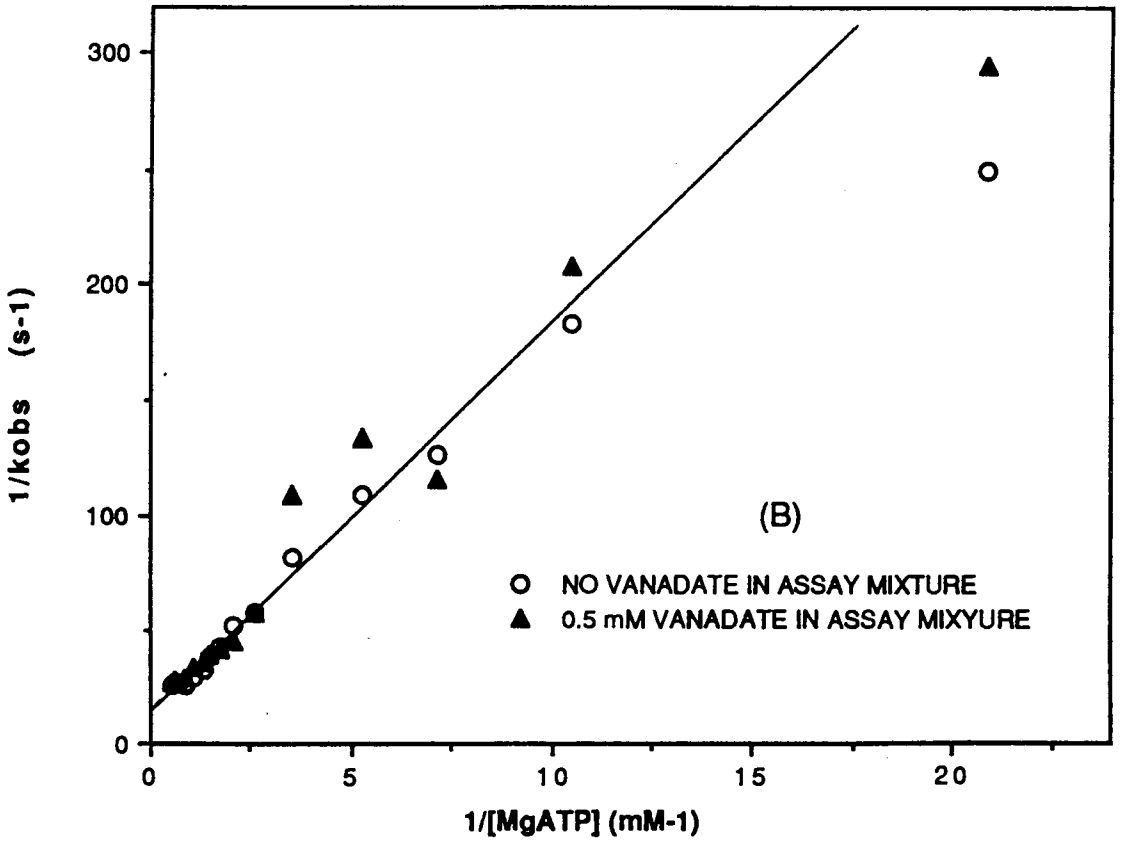
300
200
100
0
1/kobs (s-1)
0
5
10
15
20
1/[MgATP] (mM-1)
(B)
NO VANADATE IN ASSAY MIXTURE
0.5 mM VANADATE IN ASSAY MIXYURE

Figure 22. **Apparent rate constant for dissociation of vanadate from F_1 as a function of substrate ATP concentration.**

F_1 was prepared as [3,0] and at a concentration of 0.5 mg/mL. The enzyme was incubated with 100 μM vanadate for 2 hours before diluting 4 μL of the incubation mixture into 1496 μL assay solution similar to that described in Figure 20.

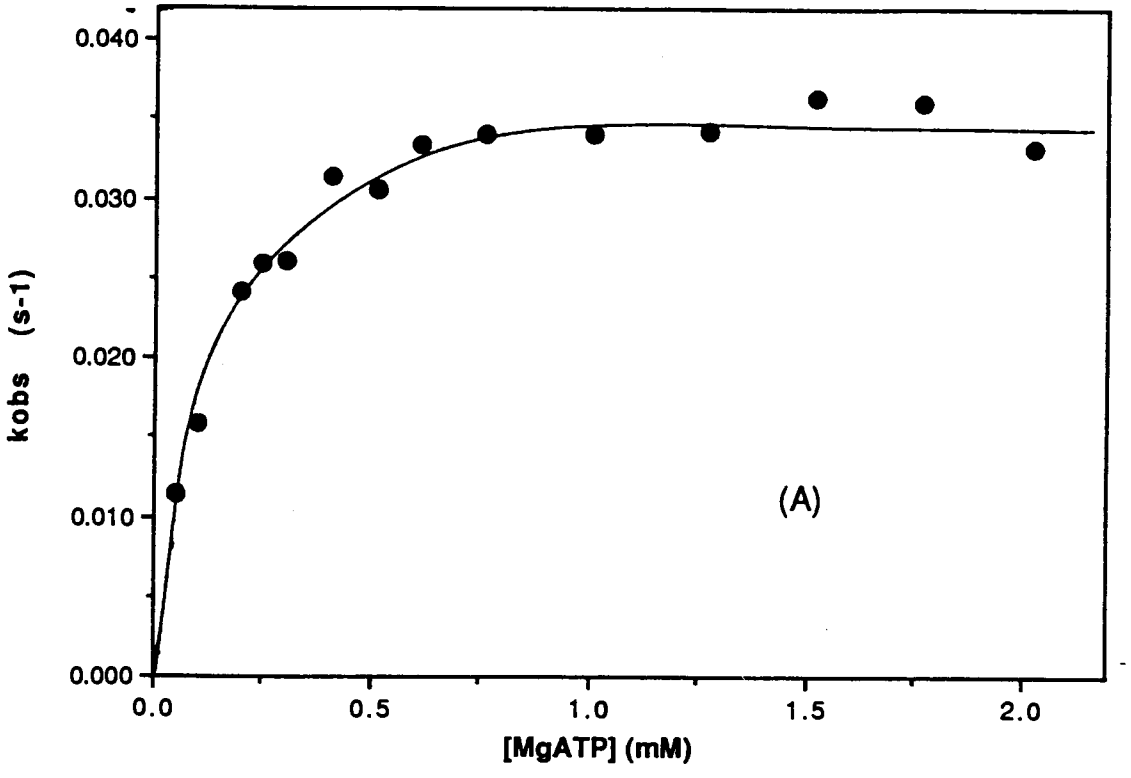
0.040
0.030
0.020
0.010
0.000
kobs (s-1)
(A)
0.0
0.5
1.0
1.5
2.0
[MgATP] (mM)

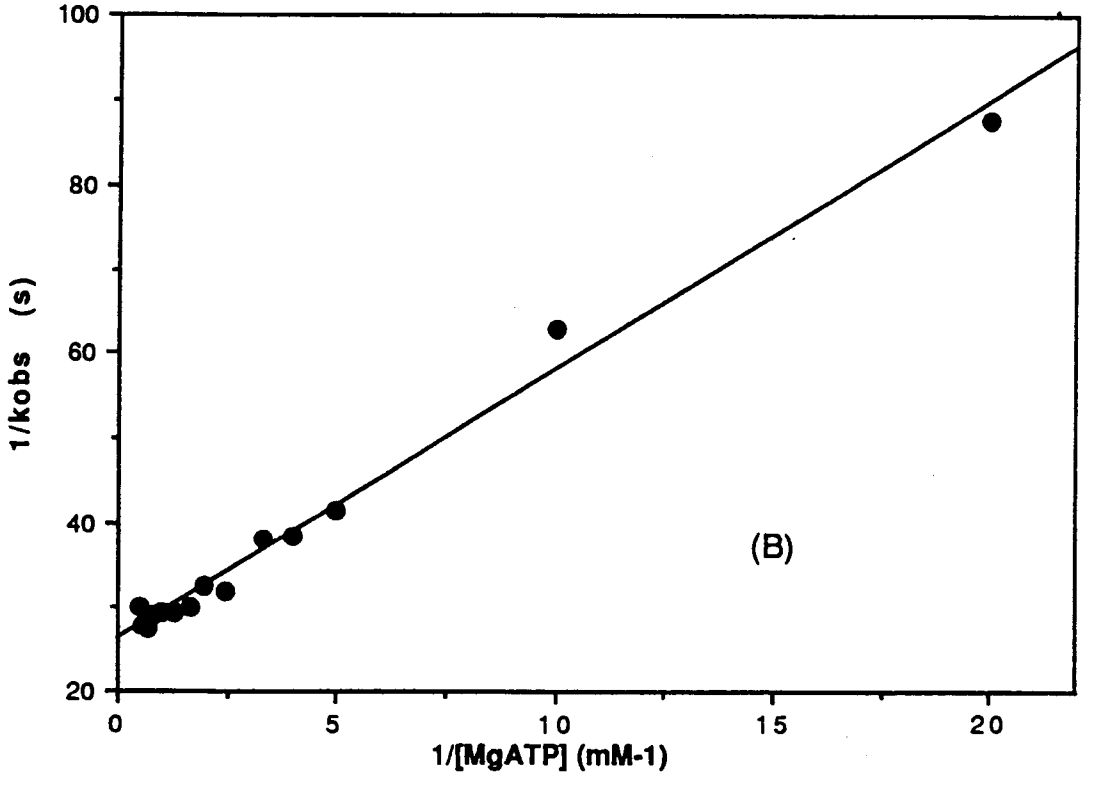
100
80
60
40
20
1/kobs (s)
(B)
0
5
10
15
20
1/[MgATP] (mM-1)

Figure 23. **Corrected apparent rate constant of dissociation of vanadate from F_1.**

Data from Figure 21 were corrected for discrepancy due to intrinsic k_{obs} obtained from the lag in the ATPase activity of F_1 used. The k_{obs} obtained from diluting F_1 + vanadate mixture into assay mixture without vanadate was substracted by 0.0021 s^{-1} while the data for enzyme diluted into assay mixture with 0.5 mM vanadate was reduced by 0.0016 s^{-1}. Graph (A) shows the corrected data in the form of a plot of k_{obs} vs. [MgATP] while (B) shows the data in the form of a double reciprocal plot.

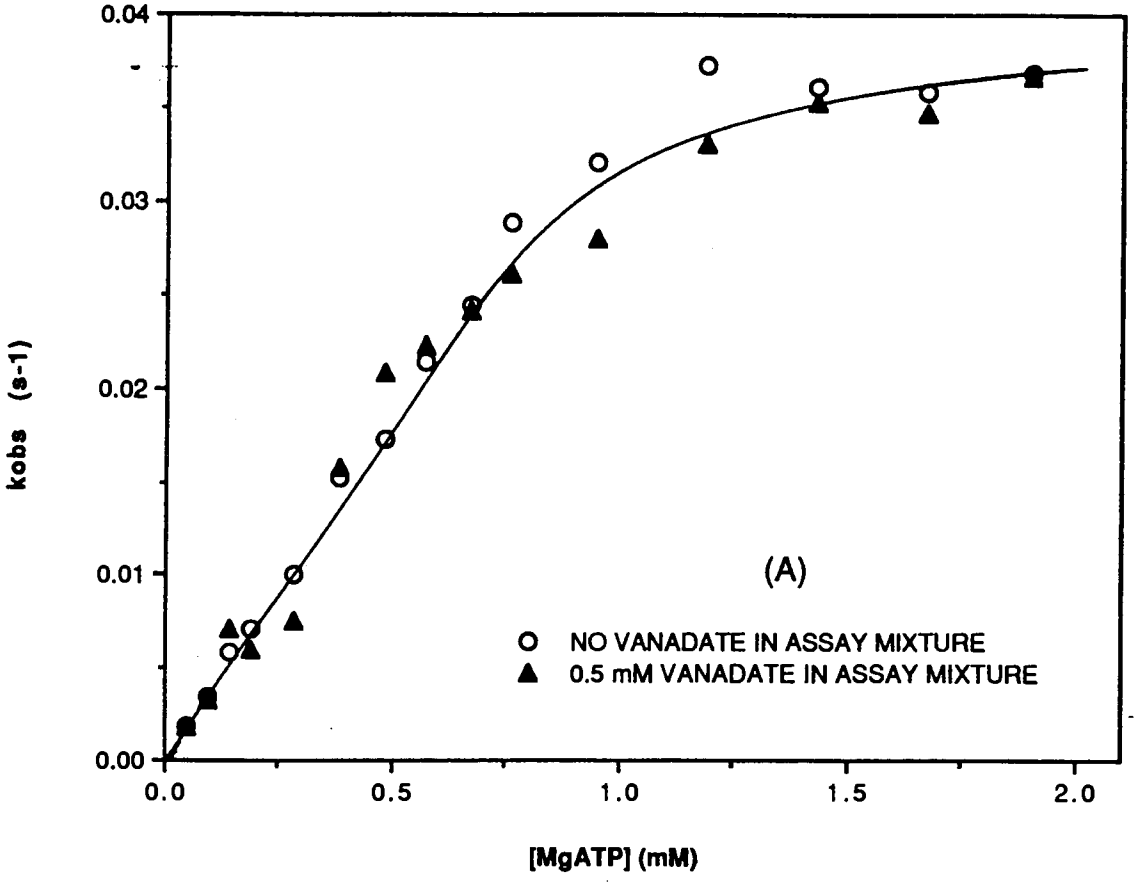
0.04
0.03
0.02
0.01
0.00
kobs (s-1)
0.0
0.5
1.0
1.5
2.0
[MgATP] (mM)
(A)
NO VANADATE IN ASSAY MIXTURE
0.5 mM VANADATE IN ASSAY MIXTURE

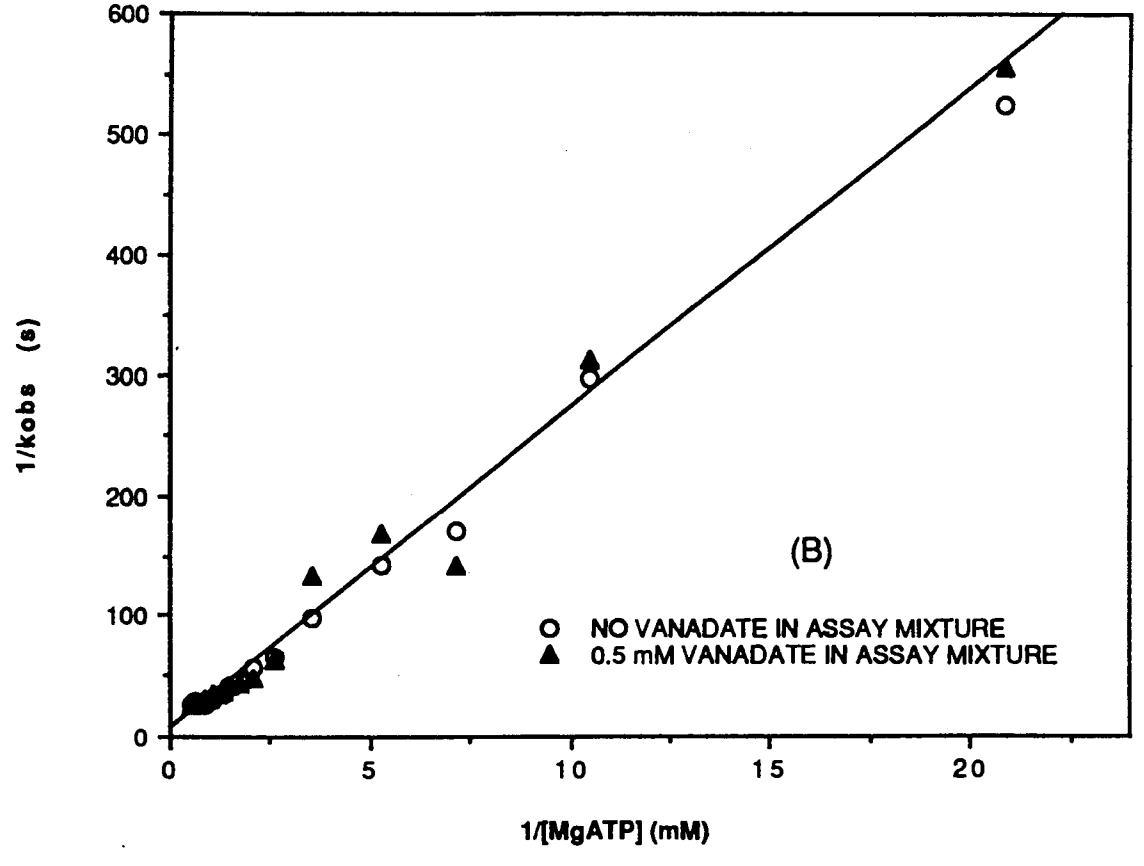
600
500
400
300
200
100
0
1/kobs (s)
0
5
10
15
20
1/[MgATP] (mM)
(B)
NO VANADATE IN ASSAY MIXTURE
0.5 mM VANADATE IN ASSAY MIXTURE

respectively. After substracting these values from the corresponding set of data, the corrected k_{obs} values were graphed in Figure 23A and 23B.

A model shown in Figure 24 is proposed to describe the interaction of vanadate with F_1 during catalysis:

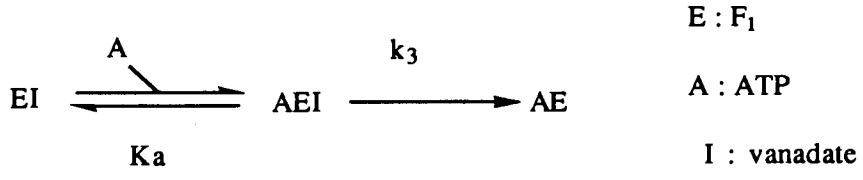

Figure 24

Model for dissociation of vanadate from F_1

Since the measurements were made in the pre-steady state,

$$(1)\quad \frac{d[AE]}{dt} = k_3[AEI] = \frac{d([EI] + [AEI])}{dt}$$

$$(2)\quad [AE] = E_T - [AEI] - [EI]$$

If association of substrate ATP with F_1-vanadate complex is assumed to be in equilibrium, K_a can be defined as:

$$(3)\quad K_a = \frac{[A][EI]}{[AEI]}$$

$$(4)\quad [EI] = [AEI]\frac{K_a}{[A]}$$

Substituting equation (4) into equation (2),

$$(5)\quad [AE] = E_T - [AEI]\left(1 + \frac{K_a}{[EI]}\right)$$

$$(6)\quad [AEI] = \frac{E_T - [AE]}{1 + \frac{K_a}{[A]}}$$

Substituting equation (6) into equation (1) gives equation (7) which can be rearranged to give equation (8).

$$(7)\quad \frac{d[AE]}{dt} = \frac{k_3 E_T}{1+\frac{K_a}{[A]}} - \frac{k_3[AE]}{1+\frac{K_a}{[A]}}$$

The apparent dissociation rate constant, k_{obs} is:

$$(8)\quad k_{obs} = \frac{k_3}{1+\frac{K_a}{[A]}}$$

$$(9)\quad \frac{1}{k_{obs}} = \frac{1}{k_3} + \frac{K_a}{k_3[A]}$$

Equation (9) expresses kobs in terms of K_a, k_3, and substrate concentration. This equation can be fitted to the data in Figure 23 using the BMDP program to find the values for the constants; k_3 was determined to be 0.062 ± 0.04 s while K_a was found to be 1.1 ± 0.2 mM. The same constants obtained from the data in Figure 22 were k_3 = 0.038 ± 0.001 s and K_a = 0.12 ± 0.01 mM^{-1}. The deviation in the K_a values may be a result of

different total incubation time (preincubation + time elapsed during experiment) during which transformation of enzyme-vanadate complex to an inactive state had occurred.

DISCUSSION

Vanadate is capable of both inhibiting F_1-ATPase during the enzyme turnover and sensitizing the enzyme to photoinactivation upon UV irradiation at 365 nm. The photoinactivation did not follow first order kinetics that is common in the photoaffinity labeling or site-specific modification of F_1. Since the control also lost partial activity after prolonged exposure to the UV illumination (Figure 2, □ and ◊), the extent of photoinactivation with long exposure time may not reliably reflect the extent of photoinactivation sensitized by vanadate. Dynein ATPase appeared to be more resistant to photodamage by UV light at the same wavelength although the sensitivity to vanadate-induced photoinactivation was comparable to that of F_1 (29). The instability of F_1 during exposure to UV light was documented by Chávez and Cuéllar (57). They reported that photodamage was most severe with UV wavelength below 300 nm; with illumination at 365 nm, the enzyme lost approximately 25% activity compared with the activity of enzyme exposed to light with λ of 550 nm. However, their irradiation conditions were different from those used in this study; the extent of photodamage thus cannot be compared. Nonetheless, their results indicated that the observed loss of enzyme activity after the exposure to UV irradiation in the absence of vanadate was not an artifact.

Results from the electrophoresis of photoinactivated F_1 suggest the possibility for the β subunits of F_1 to be either cleaved or modified as vanadate-sensitized photoinactivation of the enzyme occurred. However, the appearance of P_1 and P_2 bands on the SDS gel might also be due to the modification of γ and δ subunits because the mobility of P_1 and P_2 were very similar to that of γ and

δ subunits respectively. Experimental data obtained so far cannot confirm the origin(s) of the two new peptides on SDS gel. It is appealing to consider the these two peptides as the photocleavage products of β subunits because they contain the catalytic sites of F_1 as well as the P_i binding site where vanadate is likely to occupy when it associates with F_1. Furthermore, the β subunits were photomodified when the enzyme was photoinactivated. This phenomenon may be comparable with myosin ATPase where the site of modification and cleavage occurred on the same catalytic chain of the enzyme (32). The following discussion will base on the assumption that photocleavage of β subunits in F_1 takes place during the photoinactivation process.

In the investigation of photoinactivation of myosin ATPase in presence of vanadate, Yount and his coworkers found that the photooxidation of serine preceeded peptide cleavage; they were able to manipulate the experimental conditions such that photooxidation could be terminated before any cleavage occurred. Such control was not attained in this study with F_1-ATPase. The success in controlling the photoinactivation of myosin ATPase may be attributed to: (1) strong binding of Vi to myosin ATPase together with ADP such that the enzyme complex (E*ADP*Vi*Mg) is stable after removing unbound ligands from the enzyme; (2) the use of high intensity UV light (450 watt). In the case of F_1, when unbound vanadate was separated from the enzyme by Sephadex column centrifugation, the resulting enzyme mixture (that should contain a nearly equimolar amount of vanadate assuming the binding ratio is 1) was not photoinactivated after 30 minutes irradiation. Remaining activity of this treated enzyme was comparable with that of enzyme which had not been exposed to vanadate. This is not surprising since K_i for photoinactivation of F_1 by Vi was 12.3 $\pm$ 0.9 μM (Figure 5C). Removal of

unbound ligand from F_1 at concentrations below this would result in the dissociation of the bound ligand. Photooxidized myosin ATPase released bound Vi and photocleavage of the protein required Vi to rebind to the enzyme. With short periods of exposure to UV irradiation (4 min for myosin ATPase) and a stoichiometric amount of Vi in the mixture, chances for the rebinding of Vi were lower and the cleavage could be avoided. With F_1, however, a higher [Vi] and longer exposure to irradiation were required. Both conditions increased the chance for photocleavage to take place and hence the failure to obtain photomodified F_1 without protein cleavage.

Although enzyme incubated without vanadate or that with phosphate but no vanadate lost partial activity after exposing to UV irradiation for more than 30 minutes (Figure 2), the loss in activity was not concurrent with cleavage of the protein that was detectable on SDS-PAGE. The UV lamp has weak emmission at the lower UV wavelength which may have caused photodamage to F_1 in addition to that caused by light at 365 nm. UV light at 260 nm is known to alter aromatic side chains of amino acid residues in proteins (58); it is not established in this study, however, whether the photodamage was imposed on the same amino acid residue(s) that were photomodified in the presence of vanadate. Presence of P_i did not protect the enzyme from this photodamage nor did it sensitize the enzyme to photoinactivation; vanadate-sensitized photoinactivation of F_1 is thus a specific process that requires vanadate.

The irreversibility of photomodification of F_1 could be explained by: (1) modified site was not accessible to $NaBH_4$; (2) modified residue was not reactive toward $NaBH_4$, or (3) the modified amino acid residue was reduced but not to the same moiety as the native functional group. The latter possibility was

unlikely since pI of the β'2 was not changed by $NaBH_4$ (unless the reduction was not accompanied by a change in pI of the protein). There is no documented report on the interaction of $NaBH_4$ with F_1 nor the identification of serine as a functional amino acid residue required for its enzyme activity. In the region recognized as the possible active site of the enzyme or its vicinity, β-311 Tyr had been labeled with 8-azido ATP (28), Nbf-Cl (59, 60) and ANPP (24), while β-345 Tyr was labeled with FSBI (19) and 2-azido ADP (61). With 2-azido-ADP, β-368 Tyr was photolabeled at the noncatalytic site; FSBA also modified the enzyme at this residue (62). Since tyrosine carries a hydroxyl group similar to serine, this residue might be a target for vanadate-sensitized photooxidation. Evidence supporting the occurrence of photooxidation during F_1 photoinactivation is the participation of molecular oxygen in the process; the enzyme mixture with oxygen removed from the resuspending buffer was photoinactivated to a lesser extent (Table IV).

Table IV

Vanadate-sensitized photoinactivation of F_1 in deoxygenated medium*

Samples exposed to UV	Remaining Activity†
F_1	0.87
F_1+Vi	0.26
F_1 (deoxygenated)	0.88
F_1 + Vi (deoxygenated)	0.56

* Experimental condition and procedure as described in methods.

† Remaining activity was the ratio of activities of enzyme samples exposed and not exposed to UV irradiation.

The role of the tyrosine residues at the active site is not clearly understood. A recent study with F_1-ATPase from thermophilic bacterum PS3 (TF_1) involved substituting tyrosine at the adenine nucleotide binding sites on the β subunits (corresponding to β-311 on F_1) with Phe or Cys (63). The mutant β subunit reconstituted with α subunits forming a $\alpha_3\beta_3$ complex, which is the catalytic core of the TF_1 ATPase (64), and was able to hydrolyze ATP. The authors thus suggested that Tyr at the nucleotide binding sites are not essential for enzyme activity, in spite of the fact that the residue is conserved in various types of ATPases investigated by Walker et al (4, 5).

Direct sequencing of the N-terminal of the P_1 peptide failed to identify its origin because the N-terminal was ragged. It is unclear whether the raggedness was intrinsic or due to nonspecific cleavage. The protection of F_1 against photoinactivation by ADP and the dual effects of PP_i on the photoinactivation indicated that Vi occupies the P_i binding site on the protein since these two ligands influence P_i binding in similar manner. However, in view of the fact that P_i and Vi can bind simultaneously to F_1, a possible situation that can account for the nonspecific cleavage, if it had occurred, is Vi being capable of binding at different regions of the active site on the protein. The ability of Vi to inhibit dynein ATPase, myosin ATPases, and P_i binding to F_1 were attributed to its stability in a pentacoordinate geometry (34, 35, 47). Since γ-phosphate is the phosphate moiety of ATP molecule that passes transiently through a pentacoordinated state during enzyme catalysis, it would be reasonable for Vi to favour binding at this position in the catalytic site. This phenomenon is not unique to Vi; the fluoroaluminate (AlF_4^-) ion in which the Al can adopt a pentacoordinate geometry easily is also thought to occupy the γ-

phosphoryl position of ATP when it associates with F_1 in the presence of ADP to form an irreversibly inhibited enzyme complex (65). Vi also exists in a tetrahedral conformation and when such a geometry is adopted by the ion, it may be able to take up any of the three locations corresponding to regions usually occupied by α, β and γ phosphate of the ATP molecule. The occupation may be transitory, but nonetheless long enough for vanadate-sensitized photocleavage to take place, resulting in the observed peptide scission at possibly adjacent residues on the β-subunits.

The positions of P_1, P_2 bands on SDS gel, and $\beta'1$, $\beta'2$ bands on IEF gel were unchanged with P_i and Vi present at the same time. The IEF gel of photoinactivated F_1 shown in Figure 7 revealed the formation of two types of modified β subunit having different pI. It is not clear whether this difference in pI was due to (1) their origin of β subunits (β subunits of three different pI values were resolved on the IEF gel), (2) a result of nonspecific modification, or (3) different number of residues (for example, 1 or 2 Tyr residues on the same subunits) were modified. Although it has not been established that the possible cleavage of the β subunits of F_1 was at the same site where modification had taken place, a closer look at the results of photoinactivation of myosin ATPase may give some hint of the answer to this question. The fact that photooxidized myosin ATPase released bound Vi and that the cleavage required retrapping of Vi, indicated strongly that distinct sites of different affinity for Vi were involved.

The vanadate concentration dependence of the photoinactivation of F_1 revealed that monovanadate was the sensitizer involved. Data from $^{32}P_i$ binding experiment can be fitted with a model in which Vi can bind to F_1

alone or with P_i. The equilibrium constant for dissociation of the F_1-vanadate complex was 15.2 ± 3 μM which is in agreement with the K_i of 12.3 ± 0.9 μM obtained from the photoinactivation study. It should be pointed out that although P_i was less efficient than ADP and PP_i in protecting F_1 from photoinactivation, it still alleviated the process (Figure 10). This limited protection was obtained with a P_i concentration less than 0.5 mM; increasing $[P_i]$ to 10 mM did not provide more protection. The result is thus comparable to the inhibition of $^{32}P_i$ binding to F_1 by Vi (Figure 11) where $^{32}P_i$ binding was not abolished by high vanadate concentration. Both cases led to the conclusion that Vi and P_i can bind the enzyme simultaneously. It may be possible to investigate in more detail the P_i effect on the photoinactivation at $[P_i] < 0.5$ mM, and obtain results similar to those obtained by studying inhibition of $^{32}P_i$ binding by vanadate ion that can be explained by the interactions described in model 1.

Although monovanadate ion was the sensitizer responsible for photoinactivation of F_1, its inhibitory role in the F_1-catalyzed ATP hydrolysis was not clearly defined in this study. According to the investigation done by Bramhall (47), inhibition of F_1-ATPase activity at low vanadate concentration (< 250 μM) was attributable to Vi since the double reciprocal plot of % activity vs vanadate concentration was linear in the range between 10 - 250 μM. Deviation of data from this linear relationship was observed for higher vanadate concentrations. The inhibition of F_1-ATPase activity was investigated in this study over a wider and higher vanadate concentration range from 0.13 mM to 2.67 mM (Figures 15). It may be implied from the secondary plot shown in figures 16A-D that the number of species of vanadate(V) ions involved in the inhibition was more than one since no straight line was obtained in any of

the graphs. Another possible interpretation of the result is that the inhibition pattern changed as more than one molecule of a particular species of vanadate bound to the enzyme. The presence of a mixture of inhibitors at high vanadate concentration may explain the results in Figure 15 where the regression lines for vanadate concentration higher then 1.0 mM did not converge at the common point as the regression lines corresponding to the lower inhibitor concentrations. Furthermore, a portion of the data in figures 16B-D was linear with respect to the concentration of various vanadate species. For Vi and V_2 (Figure 16C, D), this occurred at low concentration range; for V_4 (Figure 16D), this occurred at high total vanadium atom concentration range. Combining these observations with the results from Vi-sensitized photoinactivation of F_1, inhibition of ^{32}Pi binding to F_1 by Vi, and enhancement of vanadate induced inhibition of F_1-ATPase activity in presence of P_i, both Vi and V_2 appeared likely to be involved in this kinetic inhibition at lower vanadate concentration range. Figure 16D, on the other hand, provides evidence that V_4 is the inhibitor at high vanadate concentration; however, there are other situations that can lead to this observation: (1) four Vi molecules were involved in the inhibition with high binding cooperativity, or (2) two V_2 molecules were involved at high inhibitor concentration. These situations are not unlikely because of the presence of multiple active sites on the enzyme.

The enhancement of vanadate inhibition of ATP hydrolysis by P_i should be discussed in greater detail at this point. It seems possible that the increase in vanadate inhibition of ATP hydrolysis is a result of enhanced F_1 affinity for vanadate by P_i. However, this argument received no support from the observations that: (1) P_i did not enhance Vi-sensitized photoinactivation of F_1, and (2) the extent of increase in inhibition was not proportional to the amount

of vanadate present (Figure 20B). A better explanation for the P_i promoted vanadate inhibition is the formation of inhibitory P-V anhydride. The observation that the extent of P_i enhanced vanadate inhibition was not proportional to the vanadate concentration above 1 mM can be rationalized in terms of multiple inhibitors present in the solution. P-V increases with [Vi] (P_i + Vi $\Leftrightarrow$ P-V) which is in turn dependent on the total vanadate ([V]) present in the assay mixture. V_2 and V_4 do not exist in significant quantities at low [V]. Figures 13A and 13B show that the increment of V_2 is nearly linear with respect to [V]; V_4, on the other hand, has a higher rate of increment (slope of V_4 line in Figure 13A, B becomes steeper) above 0.75 mM [V]. If V_4 is the inhibitor of F_1, its inhibitory effect is likely to be manifested more distinctly as a concentration dependent phenomenon above [V] of 0.75 mM. The rate of [Vi] increment with respect to [V] is rapid initially at low [V] but progressively becomes slower as [V] increases. As mentioned earlier, P-V formation is dependent on [Vi]; P-V concentration thus will increase at a slower pace with respect to [V] at higher concentration of V atom. The combining effect of differential rates of increment of [P-V] and [V_4] may lead to the result shown in Figure 20B. The P_i enhancement of inhibition was obscurred by the inhibition due to V_4 at higher [V]. In addition, the contention that V_4 at [V] > 0.75 mM is the predominant inhibitor of F_1 is supported by the linearity of the secondary slope plot in Figure 14D at high [V] region.

APPENDICES

APPENDIX 1

Equation (A)

$$y = \frac{[P]}{\frac{K_p K_{vp}(K_v+[V])}{K_v K_{vp}+K_p[V]} + [P]}$$

derivation shown in ref. (47),

and

$$K_p = \frac{[E][P]}{[EP]}$$

$$K_{vp} = \frac{[EV][P]}{[EVP]}$$

$$K_v = \frac{[E][V]}{[EV]}$$

$$y = \frac{[EP] + [EVP]}{e}$$

where e = total enzyme concentration and y is the binding ratio determined experimentally and is represented by $\frac{^{32}P_i}{F_1}$ in Figure 11.

APPENDIX 2

Derivation of the equation for determining k_{obs} of vanadate dissociation from F_1 is as follows.

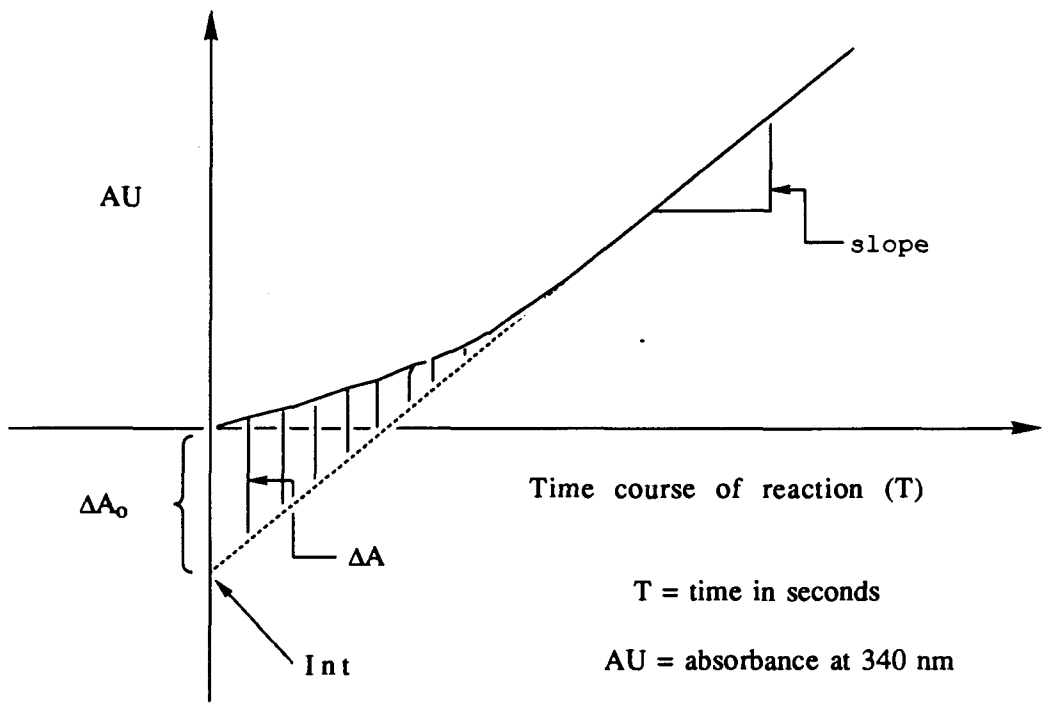

For the dissociation of vanadate from F_1 which followed a first order kinetics, the following expression was obtained.

(1) $\Delta A = \Delta A_o e^{-kT}$ where $k = k_{obs}$

From the figure shown above, equation (2) can be obtained.

(2) $\Delta A = \text{Slope} * T + \text{Int} - AU$

(3) $AU = \text{Slope} * T + \text{Int} - \Delta A$

Substituting equation (1) into equation (3) gives equation (4)

$$(4)\quad AU = Slope * T + Int - \Delta A_o e^{-kT}$$

k was assigned as P1 and ΔA_o as e^{P2} to give equation (5).

$$(5)\quad AU = Slope * T + Int - e^{P2}\, e^{P1*T}$$

$$(6)\quad AU = Slope * T + Int - e^{P1*T+P2}$$

$$(7)\quad AU = Slope * T + Int - 10^{\left(\frac{P1*T+P2}{2.303}\right)}$$

Equation (7) was the fitting equation provided to the computer for the determination of k_{obs}.

REFERENCES

(1) Hatefi, Y. (1985) Annu. Rev. Biochem. *54*, 1015-1069.

(2) Vignais, P. V., and Lunardi, J. (1985) Annu. Rev. Biochem. *54*, 977-1014.

(3) Senior, A. E. (1988) Physiol. Rev. *68*, 177-231.

(4) Runswick, M. J., and Walker, J. E. (1983) J. Biol. Chem. *258*, 3081-3089.

(5) Walker, J. E., Fearnley, I. M., Gay, N. J., Gibson, B. W., Northrop, F. D., Powell, S. J., Runswick, M. J., Saraste, M., and Tybulewicz, V. L. J. (1985) J. Mol. Biol. *184*, 677-701.

(6) Lünsdorf, H., Ehrig, K., Friedl, P., and Schairer, H. U. (1984) J. Mol. Biol. *173*, 131-136.

(7) Tiedge, H., Lünsdorf, H., Schafer, G., and Schairer, H. U. (1985) Proc. Natl. Acad. Sci. U.S.A. *82*, 7874-7878.

(8) Cross, R. L., and Nalin, C. M. (1982) J. Biol. Chem. *257*, 2874-2881.

(9) Weber, J., Lücken, U., and Schafer, G. (1985) Eur. J. Biochem. *148*, 41-47.

(10) Issartel, J. -P., Farre-Bulle, O., Lunardi, J., and Vignais, P. V. (1987) J. Biol. Chem. *262*, 13538-13544.

(11) Penefsky, H. S. (1977) J. Biol. Chem. *252*, 2891-2899.

(12) Kasahara, M., and Penefsky, H. S. (1978) J. Biol. Chem. *253*, 4180-4187.

(13) Pullman, M. E., and Monroy, G. C. (1963) J. Biol. Chem. *238*, 3762-3769.

(14) Pederson, P. L., Schwerzmann, K., and Cintron, N. (1981) Curr. Top. Bioenerg. *11*, 149-199.

(15) Klein, G., Satre, M., Dianoux, A. -C., and Vignais, P. V. (1980) Biochem. *19*, 2919-2925.

(16) Wang, J. H. (1985) J. Biol. Chem. *260*, 1374-1377.

(17) Pedersen, P. L., and Amzel, M. (1985) in *Achievements and Perspectives of Mitochondrial Research. Vol. I : Bioenergetics*, eds. Quagiariells, E. et al. (Elservier, Amsterdam), pp. 169-189.

(18) Bullough, D. A., and Allison, W. S. (1986) J. Biol. Chem. *261*, 14171-14177.

(19) Cross, R. L. (1981) Annu. Rev. Biochem. *50*, 681-714.

(20) Gresser, M. J., Myers, J.A., and Boyer, P. D. (1982) J. Biol. Chem. *257*, 12030-12038.

(21) Sakamoto, J., and Tonomura, Y. (1983) J. Biochem. *93*, 1601-1614.

(22) Lanquin, G. J. -M., Pougeosis, R., and Vignais, P. V. (1980) Biochem. *19*, 4620-4626.

(23) Pougeosis, R., and Lanquin, G. J. -M. (1985) Biochem. *24*, 1020-1024.

(24) Garin, J., Michel, L., Dupuis, A., Issartel, J. -P., Lunardi, J., Hoppe, J., and Vignais, P. V. (1989) Biochem, *28*, 1442-1228.

(25) Pougeois, R., Lanquin, G., and Vignais, P. V. (1983) FEBS Lett. *153*, 65-70.

(26) Pougeois, R., Lanquin, G., and Vignais, P. V. (1983) Biochem. *22*, 1241-1245.

(27) Hollemans, M., Runswick, M. J., Fearnley, I. M., and Walker, J. E. (1983) J. Biol. Chem. *258*, 9307-9313.

(28) Lee-Eiford, A., Ow, R. A., and Gibbons, I. R. (1986) J. Biol. Chem. *261*, 2337-1342.

(29) Gibbons, I. R., Lee-Eiford, A., Mocz, G., Phillipson, C. A., Tang, W. -J. Y., and Gibbons, B. H. (1987) J. Biol. Chem. *262*, 2780-2786.

(30) Tang, W. -J. Y., and Gibbons, I. R. (1987) J. Biol. Chem. *263*, 17728-17734.

(31) Grammer, J. C., Cremo, C. R., and Yount, R. G. (1988) Biochem. *27*, 8408-8415.

(32) Cremo, C. R., Grammer, J. C., and Yount, R. G. (1988) Biochem. *27*, 8415-8420.

(33) Mogel, S. N., and Bruce, A. M. (1989) Biochem. *28*, 5438-5431.

(34) Gibbons, I. R., Cosson, M. P., Evans, J. A., Gibbons. B. H., Houke, B., Martinson, K. H., Sale, W. S., and Tang, W. -J. Y. (1978) Proc. Natl. Acad. Sci. U.S.A. *75*, 2220-2224.

(35) Goodno, C. C. (1979) Proc. Natl. Acad. Sci. U.S.A. *76*, 2620-2624.

(36) Meusch, H. -U., and Bielig, H. -J. (1980) Basic Res. Cardiol. *75*, 413-417.

(37) Chasteen, N. D. (1983) Struct. Bond. *53*, 106-138.

(38) Knowles, A. F., and Penefsky, H. S. (1972) J. Biol. Chem. *247*, 6617-6623.

(39) Cross, R. L., Cunningham, D., and Tamura, J. K. (1984) Curr. Top. Cell. Regul. *24*, 335-344.

(40) Cunninigham, D., and Cross, R. L. (1988) J. Biol. Chem. *263*, 18850-18856.

(41) Lowry, O. H., Rosebrough, N. J., Farr, A. L., and Randall, R. J. (1951) J. Biol. Chem. *193*, 265-275.

(42) Hartree, E. F. (1972) Anal. Biochem. *48*, 422-427.

(43) Laemmli, U. K. (1970) Nature, *227*, 680-685.

(44) O'Farrell, P. H. (1975) J. Biol. Chem. *250*, 4007-4021.

(45) O'Farrell, P. Z., Goodman, H. M., and O'Farrell, P. H. (1977) Cell, *12*, 1133-1142.

(46) Beharry, S., and Gresser, M. J. (1987) J. Biol. Chem. *262*, 10630-10637.

(47) Bramhall, E. (1987) M. Sc. Thesis, Simon Fraser University.

(48) Gresser, M. J., and Tracey, A. S. (1985) J. Am. Chem. Soc. *107*, 4215-4220.

(49) Tracey, A. S., and Gresser. M. J. (1986) Proc. Natl. Acad. Sci. U. S. A. *83*, 609-613.

(50) Ferguson, J. H., and Kustin, K. (1979) Inorg. Chem. *18*, 3349-3357.

(51) Tracey, A. S., Gresser, M. J., and Parkinson, K. M. (1987) Inorg. Chem. *26*, 629-638.

(52) Tracey, A. S., Gresser, M. J., and Liu, S. (1988) J. Am. Chem. Soc. *110*, 5869-5874.

(53) Darr, D., and Fridovich, I. (1984) Arch. Biochem. Biophys. *232*, 562-565.

(54) Kastelic, T. (1987) M. Sc. Thesis, Simon Fraser University.

(55) Wilkinson, G. N. (1961) Biochem. J. *80*, 324-332.

(56) Gresser, M. J., Tracey, A. S., and Parkinson, K. M. (1986) Am. Chem. Soc. *108*, 6229-6234.

(57) Chávez, E., and Cuéllar, A. (1984) Arch. Bioch. Biophys. *230*, 511-516.

(58) Crossweiner, L. T., and Usui, Y. (1970) Photochem. Photobiol. *11*, 53-56.

(59) Andrews, W. W., Hill, F. C., and Allison, W. S. (1984) J. Biol. Chem. *259*, 8219-8225.

(60) Sutton, R., and Ferguson, S. J. (1985) Eur. J. Biochem. (1985) *148*, 551-554.

(61) Cross, R. L., Cunningham, D., Miller, C. G., Xue, Z., Zhou, J. -M., and Boyer, P. D. (1987) Proc. Natl. Acad. Sci. U. S. A. *84*, 5715-5719.

(62) Esch, F., and Allison, W. S. (1978) J. Biol. Chem. *253*, 6100-6106.

(63) Odaka, M., Kobayashi, H., Muneyeki, E., and Yoshida, M. (1990) Bioch. Biophys. Res. Commun. *168*, 372-378.

(64) Miwa, K., and Yoshida, M. (1989) Proc. Natl. Acad. Sci. U.S.A. *86*, 6484-6487.